



## A measurement-based verification framework for UK greenhouse gas emissions: an overview of the Greenhouse gAs Uk and Global Emissions (GAUGE) project

Paul I. Palmer<sup>1</sup>, Simon O'Doherty<sup>2</sup>, Grant Allen<sup>3</sup>, Keith Bower<sup>3</sup>, Hartmut Bösch<sup>4</sup>, Martyn P. Chipperfield<sup>5</sup>, Sarah Connors<sup>7</sup>, Sandip Dhomse<sup>6</sup>, Liang Feng<sup>1,8</sup>, Douglas P. Finch<sup>1</sup>, Martin W. Gallagher<sup>3</sup>, Emanuel Gloor<sup>6</sup>, Siegfried Gonzi<sup>1,9</sup>, Neil R. P. Harris<sup>10</sup>, Carole Helfter<sup>11</sup>, Neil Humpage<sup>4</sup>, Brian Kerridge<sup>12,13</sup>, Diane Knappett<sup>12,13</sup>, Roderic L. Jones<sup>7</sup>, Michael le Breton<sup>3,14</sup>, Mark F. Lunt<sup>2</sup>, Alistair J. Manning<sup>15</sup>, Stephan Matthiasen<sup>1</sup>, Jennifer B.A. Muller<sup>3,16</sup>, Neil Mullinger<sup>11</sup>, Eiko Nemitz<sup>11</sup>, Sebastian O'Shea<sup>3</sup>, Robert J. Parker<sup>4</sup>, Carl J Percival<sup>3,17</sup>, Joseph Pitt<sup>3</sup>, Stuart N. Riddick<sup>7</sup>, Matthew Rigby<sup>2</sup>, Harjinder Sembhi<sup>4</sup>, Richard Siddans<sup>12,13</sup>, Robert L. Skelton<sup>7</sup>, Paul Smith<sup>7,18</sup>, Hannah Sonderfeld<sup>4</sup>, Kieron Stanley<sup>2</sup>, Ann R. Stavert<sup>2</sup>, Angelina Wenger<sup>2</sup>, Emily White<sup>2</sup>, Christopher Wilson<sup>5,19</sup>, and Dickon Young<sup>2</sup>

<sup>1</sup>School of GeoSciences, University of Edinburgh, UK

<sup>2</sup>School of Chemistry, University of Bristol, UK

<sup>3</sup>Centre for Atmospheric Science, The University of Manchester, Manchester, UK

<sup>4</sup>Earth Observation Science Group, Department of Physics and Astronomy, University of Leicester, Leicester, UK

<sup>5</sup>School of Earth and Environment, University of Leeds, Leeds, UK

<sup>6</sup>School of Geography, University of Leeds, Leeds, UK

<sup>7</sup>Centre for Atmospheric Science, University of Cambridge, Cambridge, UK

<sup>8</sup>National Centre for Earth Observation, University of Edinburgh

<sup>9</sup>Now at the Met Office, Exeter, UK

<sup>10</sup>Centre for Environmental and Agricultural Informatics, Cranfield University, Cranfield, UK

<sup>11</sup>Centre for Ecology and Hydrology, Penicuik, UK

<sup>12</sup>Space Science and Technology Department, Rutherford Appleton Laboratory, Oxfordshire, UK

<sup>13</sup>National Centre for Earth Observation, Rutherford Appleton Laboratory, UK

<sup>14</sup>Now at Department of Chemistry & Molecular Biology, University of Gothenburg, Gothenburg, Sweden

<sup>15</sup>Met Office, Exeter, UK

<sup>16</sup>Now at Deutscher Wetterdienst, Meteorologisches Observatorium Hohenpeißenberg, Hohenpeißenberg, Germany

<sup>17</sup>Now at the Jet Propulsion Laboratory, Pasadena, CA, USA

<sup>18</sup>Now at Institute of Physical Chemistry Rocasolano, Madrid, Spain

<sup>19</sup>National Centre for Earth Observation, University of Leeds, UK

Correspondence to: P. I. Palmer  
([paul.palmer@ed.ac.uk](mailto:paul.palmer@ed.ac.uk))



**Abstract.** We describe the motivation, design, and execution of the Greenhouse gAs Uk and Global Emissions (GAUGE) project. The overarching scientific objective of GAUGE was to use atmospheric data to estimate the magnitude, distribution, and uncertainty of the UK greenhouse gas (GHG, defined here as CO<sub>2</sub>, CH<sub>4</sub>, and N<sub>2</sub>O) budget, 2013-2015. To address this objective we established a multi-year and interlinked measurement and data analysis programme, building on an established tall tower GHG measurement network. The inter-calibrated measurement network comprises ground-based, airborne, ship-borne, balloon-borne, and space-borne GHG sensors. Our choice of measurement technologies and measurement locations reflects the heterogeneity of UK GHG sources that range from small point sources such as landfills to large, diffuse sources such as agriculture. Atmospheric mole fraction data collected at the tall towers and on the ships provide information on sub-continental fluxes, representing the backbone to the GAUGE network. Additional spatial and temporal details of GHG fluxes over East Anglia were inferred from data collected by a regional network. Data collected during aircraft flights were used to study the transport of GHGs on local and regional scales. We purposely integrated new sensor and platform technologies into the GAUGE network, allowing us to lay the foundations of a strengthened UK capability to verify national GHG emissions beyond the project lifetime. For example, current satellites provide sparse and seasonally uneven sampling over the UK mainly because of its geographical size and cloud cover. This situation will improve with new and future satellite instruments, e.g. measurements of CH<sub>4</sub> from the TROPOMI instrument aboard Sentinel-5P. We use global, nested, and regional atmospheric transport models and inverse methods to infer geographically resolved CO<sub>2</sub> and CH<sub>4</sub> fluxes. This multi-model approach allows us to study model spread in *a posteriori* flux estimates. These models are used to determine the relative importance of different measurements to infer the UK GHG budget. Attributing observed GHG variations to specific sources is a major challenge. Within a UK-wide spatial context we used two approaches: 1)  $\Delta^{14}\text{CO}_2$  and other relevant isotopologues (e.g.  $\delta^{13}\text{C}_{\text{CH}_4}$ ) from collected air samples to quantify the contribution from fossil fuel combustion and other sources; 2) geographical separation of individual sources, e.g. agriculture, using a high-density measurement network. Neither of these represents a definitive approach, but they will provide invaluable information about GHG source attribution when they are adopted as part of a more comprehensive, long-term national GHG measurement programme. We also conducted a number of case studies, including an instrumented landfill experiment that provided a test-bed for new technologies and flux estimation methods. We anticipate that results from the GAUGE project will help inform other countries on how to use atmospheric data to quantify their nationally determined contributions to the Paris Agreement.



## 1 Introduction

35 Human-driven emissions of carbon dioxide (CO<sub>2</sub>), methane (CH<sub>4</sub>), nitrous oxide (N<sub>2</sub>O), and other  
greenhouse gases (GHGs) to the Earth's atmosphere perturb the balance between net incoming solar  
radiation and outgoing terrestrial radiation. These emissions, primarily from the combustion of  
fossil fuels and land-use change activities, are the dominant cause of the warming trend in the climate  
system since the 1950s (IPCC, 2013). Minimizing the manifold impacts of increasing atmospheric  
40 GHGs demands a structured timetable of emission reductions. Avoiding the two-degree Celsius  
global temperature rise (Nordhaus, 1977) requires that we are already close to peak emissions,  
with stringent reductions that lead to zero or negative net emissions by 2100. At the Paris Conference  
of the Parties (COP) in December 2015, 195 countries agreed to accelerate this schedule in  
order to achieve net zero emissions later this century. Achieving this objective demands accurate  
45 knowledge of national GHG emissions and the contributions from individual sectors. The United  
National Framework Convention on Climate Change (UNFCCC) requires that all countries included  
in Annex 1 of that Convention report their annual GHG inventory, including CO<sub>2</sub>, CH<sub>4</sub>, and N<sub>2</sub>O.  
The bottom-up approach to determining these emissions from individual sectors is on a production,  
in-use, and disposal basis using source-dependent activity data and emissions factors. A complementary  
50 top-down approach is to verify nationwide GHG emissions using atmospheric measurements of  
these GHGs, but in practice this is non-trivial and presents many scientific challenges. Here, we  
describe the UK Natural Environment Research Council (NERC) Greenhouse gAs UK and Global  
Emissions (GAUGE) project. In particular, we 1) define the scientific objectives of GAUGE; 2) describe  
individual measurement types and the atmospheric transport models used to interpret these  
55 data; and 3) outline the broader modelling approach that is adopted in order to determine the magnitude  
and uncertainty of UK flux estimates of GHGs. Throughout this paper, where relevant, we refer  
the reader to peer-reviewed publications describing the analysis of individual GAUGE datasets.

The UK Climate Change Act 2008 commits the UK to reduce GHG emissions by at least 80%  
below 1990 baseline levels by 2050, with an interim target of a 34% reduction compared the same  
60 baseline by 2020. To establish a realistic trajectory towards the 2020 and 2050 goals, the Climate  
Change Act established five five-year carbon budgets (2008–2032). Seven GHGs are the subject of  
these staged emission reductions: CO<sub>2</sub>, CH<sub>4</sub>, N<sub>2</sub>O, hydrofluorocarbons, perfluorocarbons, sulphur  
hexafluoride, and nitrogen trifluoride.

UK government statistics report that CO<sub>2</sub>, CH<sub>4</sub>, and N<sub>2</sub>O correspond to  $\approx 81\%$ , 11%, and 5% of  
65 the estimated UK 495.7 MtCO<sub>2</sub>e (budget in 2015, Department for Business Energy and Industrial  
Strategy (2017)); the remaining 3% is due to fluorinated gases. This budget, broken down by sector in  
2015: energy supply (29%), transport (24%), business (17%), residential (13%), agriculture (10%),  
waste management (4%), industrial processes (2%), and other (1%). Emissions of CO<sub>2</sub> are largest  
for energy supply, transport, business, and residential sectors. CH<sub>4</sub> emissions are largest for agricul-  
70 ture and waste management, and N<sub>2</sub>O emissions are largest for agriculture. These emission sources



are very different in nature, ranging from point sources (e.g. industry) to geographically large, diffuse sources (e.g. agriculture). We take into account these differences in the GAUGE measurement strategy, as described below.

The primary objective of GAUGE is to quantify the magnitude, distribution, and uncertainty of the UK GHG CO<sub>2</sub>, CH<sub>4</sub>, and N<sub>2</sub>O budgets, 2013–2015. Our rationale is that better understanding the national GHG budget will inform the development of effective emission reduction policies that help the UK to meet the interim targets of the UK Climate Change Act and to achieve its commitments to the Paris Agreement. To achieve our primary objective we put together a 42-month research programme, bringing together a purpose-built atmospheric measurement network and a range of atmospheric transport models and inverse methods to translate those measurements into UK GHG flux estimates. More broadly, GAUGE provides an assessment of our current ability to infer GHG fluxes from atmospheric data, and strengthens the UK capability to verify national GHG budgets beyond the lifetime of GAUGE.

GAUGE builds on a long heritage of UK atmospheric observations that have been used to estimate national GHG emissions. Manning et al. (2003) were the first to apply an inverse model approach to infer UK CH<sub>4</sub> and N<sub>2</sub>O emissions, using data collected from Mace Head (MHD), Ireland, during 1995–2000. This approach contrasted clean upwind air that arrived from the North Atlantic with air masses that passed over mainland UK and Europe and influenced by continental fluxes (Villani et al., 2010). Although, these data provided incomplete measurement coverage of the UK, results using this method have been part of the UK reporting to the UNFCCC. In later work, Polson et al. (2011) used research aircraft observations of GHG mole fractions from the NERC-funded AMPEP campaign (Aircraft Measurement of Chemical Processing and Export fluxes of Pollutants over the UK) to infer fluxes of CO<sub>2</sub>, CH<sub>4</sub>, and N<sub>2</sub>O and a range of halocarbons. During AMPEP the research aircraft circumnavigated the UK during the summer of 2005 and September 2006. They found that the inferred CO<sub>2</sub> fluxes during the campaign were close to the bottom-up emission inventory, but CH<sub>4</sub> and N<sub>2</sub>O fluxes were much larger than the inventory data but with significant uncertainties. The main advantage of using an aircraft is its ability to sample nationwide scale emissions over a relatively short time period. However limited sorties during AMPEP left gaps in sampling, which affected their ability to describe GHG emissions that include large seasonal cycles (e.g. agriculture). For more than a decade the UK has included a verification annex chapter to its annual National Inventory Report to the UNFCCC (<https://www.unfccc.int>). This chapter provides an annual comparison of the reported GreenHouse Gas Inventory (GHGI) of each reported gas to those estimated using atmospheric observations and the Bayesian inverse modelling technique InTEM (Inversion Technique for Emission Modelling). The precursor to InTEM is described by Manning et al. (2011). InTEM uses the output from the NAME (Numerical Atmospheric dispersion Modelling Environment) transport model (Manning et al., 2011), which describes how emissions disperse and dilute in the atmosphere, and observations from the UK DECC (Deriving Emissions related to Climate Change)



tall tower network (described below). A recent study used NAME and a hierarchical Bayesian approach to determined UK emissions of CH<sub>4</sub> and N<sub>2</sub>O using the UK DECC network from 2012 to  
110 2014 (Ganesan et al., 2015). They found that *a posteriori* fluxes were lower than *a priori* values. Using geographical distributions of sectoral emissions, Ganesan et al. (2015) tentatively attributed their result to an overestimation of agricultural emissions of CH<sub>4</sub>, and a significant seasonal cycle of N<sub>2</sub>O emissions. Recent work has incorporated the reversible jump Markov Chain Monte Carlo (MCMC) inverse modelling method (Lunt et al., 2016). The main advantage of this new approach  
115 is that the algorithm chooses the number of the unknown parameters, including the geographical size of the region, to be solved given the data. *A posteriori* CH<sub>4</sub> emissions for March 2014 inferred from the DECC network data were consistent with Ganesan et al. (2015) (Lunt et al., 2016). Within the GAUGE project InTEM is used together with other inverse methods (section 3) to provide an ensemble of flux estimates, which provide a broader picture of the range of estimates. Using InTEM  
120 also provides a link between GAUGE and previous UK GHG estimates.

The measurement strategy we have adopted within GAUGE includes long-term measurements and shorter-term, higher-resolution network measurements, focused aircraft experiments, CO<sub>2</sub> sondes, characterization of point sources such as landfills, and satellite remote sensing. Our approach accounts for the heterogeneity of UK sources, e.g. point sources for power generation to large, dif-  
125 fuse and seasonal sources from agriculture. It also addresses the need to focus attention on smaller regional and city scales. This focus on smaller regions will progressively grow in importance with ongoing rapid rates of urbanization across the world. GAUGE included new *in situ* and remote sensing technologies, and new measurement platforms (e.g. unmanned aerial vehicles) that will help to future-proof the UK GHG measurement network. To help attribute observed variations in at-  
130 mospheric GHGs to individual sources, e.g. fossil fuel combustion, we explored the potential of isotopologues to chemically identify source signatures, and high-density measurements to exploit geographical distributions of individual sector emissions.

In section 2 we describe the measurements we collected during GAUGE and the attributes that make them ideal for quantifying nationwide GHG fluxes. We also discuss the inter-calibration efforts  
135 that put these different data on internationally-recognized calibration scales, placing GAUGE data into a wider context. In section 3 we describe the models we use to describe atmospheric chemistry and transport, the challenges faced, and the associated inverse methods that we use to infer GHG fluxes from the GAUGE data. We conclude in section 4.

## 2 Measurements

140 We present an overview of the measurements collected as part of GAUGE in Tables 1, 2, 4, 5, 6, and 8. We distinguish between *in situ* measurements, mobile measurements platforms, and space-borne data. We also include a description of how we inter-calibrate these different data.



## 2.1 In Situ Measurements

We use tall tower measurements and the atmospheric baseline observatory at MHD to provide a  
145 long-term *in situ* measurement record to underpin the main objectives of GAUGE. Tall towers are  
used to collect atmospheric GHG measurements that are sensitive to fluxes on a horizontal scale  
of 10–100s km. We also established a geographically dense network of observations to help isolate  
GHG emissions from individual sources.

### Tall Tower Measurement Network

150 Figure 1 shows the geographical locations of the tall towers (TTs) that collect atmospheric mea-  
surements of GHGs (Tables 1 and 2) and provide the long-term, core measurement capability of the  
UK GHG measurement network. Sampling air high above the land surface reduces the influence  
of local signals that can compromise interpretation of observed variations of GHGs (Gerbig et al.,  
2003, 2009). With the exception of the MHD atmospheric research station (described below) air is  
155 typically sampled at least 50 m above the local terrain and at multiple heights (Table 1) to assess the  
role of atmospheric mixing in the planetary boundary layer.

Tables 1 and 2 describe the five TT locations and the MHD site used in the GAUGE project.  
High-frequency measurements of GHGs have been collected for the past three decades at the MHD  
northern hemisphere background measurement station on the west coast of Ireland. They predomi-  
160 nately represent clean, western baseline conditions for the UK and mainland Europe. These MHD  
data have been previously used to infer UK-wide GHG emissions (Manning et al., 2011). In 2012,  
the UK Deriving Emissions linked to Climate Climate (UK DECC) tall tower network was estab-  
lished across mainland UK using funding from the UK Department of Energy and Climate Change  
(with the responsibility now residing in the Department for Business, Energy and Industrial Strategy,  
165 BEIS). Three sites were established (Angus, Ridge Hill, and Tacolneston, Table 1) with the purpose  
of improving the spatial and temporal distribution of measurements across the UK to reduce un-  
certainties of GHG emissions for the devolved administrations (i.e. England, Wales, Scotland, and  
Northern Ireland). As part of the GAUGE project, we augmented the UK DECC network with two  
TT sites at Bilsdale and Heathfield (Figure 1) that started collecting data from 2013 onwards. These  
170 two new sites were chosen to help fill the measurement coverage over mid-northern England, where  
there is significant industrial activity, and to collect measurements south of London. For detailed  
descriptions of each site, measurement and data logging instrumentation, and the calibration proto-  
cols we refer the reader to Appendix A, Stanley et al. (2017) and A. R. Stavert et al., “GAUGE Tall  
Towers: measurements, methodologies and impact,” in preparaton for *Atmos. Chem. Phys. Discuss.*,  
175 2018 - hereafter ARS18a.

As an example, Figure 2 shows CO<sub>2</sub>, CH<sub>4</sub>, and N<sub>2</sub>O mole fraction data from Bilsdale, North  
Yorkshire. Figure 2 also shows the statistically determined baseline, long term trend and mean diur-



nal cycle for each season. The statistical fitting procedure is described in Thoning et al. (1989), and on the associated NOAA/ESRL website <http://www.esrl.noaa.gov/gmd/ccgg/mbl/crvfit/crvfit.html>.

180 The mean Bilsdale growth rates for CO<sub>2</sub>, CH<sub>4</sub> and N<sub>2</sub>O are 3 ppm/yr, 8 ppb/yr and 0.8 ppb/yr, respectively. The mean seasonal amplitudes for these gases are 18 ppm, 51 ppb, and 0.8 ppb, respectively. Table 3 summarizes the descriptive statistics for tall towers data. Diurnal variations of these gases vary seasonally, particularly CO<sub>2</sub> and CH<sub>4</sub> that have large surface fluxes. Fluxes of CO<sub>2</sub>, for instance, have a peak diurnal cycle of  $\approx 10$  ppm during summer months. Diurnal variations during

185 winter months, particularly evident at lower inlet heights, provide some indication of the role of boundary layer height. Variations of CH<sub>4</sub> are due to changes in anthropogenic emissions but also to higher summertime OH concentrations, which represent the main loss term. N<sub>2</sub>O has an atmospheric lifetime  $\approx 120$  years, determined by stratospheric photolysis. Our measurements show a growth rate that is consistent with the global value of  $\approx 0.9$  ppb/yr.

190 We also analyzed the radiocarbon content of CO<sub>2</sub> ( $\Delta^{14}\text{CO}_2$ ) at MHD and TAC as an approach to estimate the fossil fuel contribution to observed atmospheric variations of CO<sub>2</sub> (ffCO<sub>2</sub>). The underlying idea is that fossil fuels, by virtue of their age, are devoid of <sup>14</sup>C, which has a half-life of  $5700 \pm 30$  years (Roberts and Southon, 2007). Measurements of  $\Delta^{14}\text{CO}_2$  have been used extensively to determine ffCO<sub>2</sub> (e.g. Meijer et al. (1996); Levin et al. (2003); Levin and Karstens

195 (2007); Turnbull et al. (2006, 2009); Graven et al. (2009); Berhanu et al. (2017)). Our sampling strategy at MHD (nominally unpolluted site) and TAC (nominally polluted site) was designed to determine the west-east gradient of ffCO<sub>2</sub>, reflecting the prevailing wind direction over the UK.

Weekly glass flask sample pairs were collected at MHD and TAC. A commercial sampling package is used at MHD (Hermes PFP, High Precision Devices Inc., USA) as part of the National Oceanic

200 & Atmospheric Administration (NOAA) Carbon Cycle Greenhouse Gases global flask sampling program run by the Earth System Research Laboratory (ESRL). Flask pairs have been filled at MHD for NOAA since 1991, but they have not been previously analysed for <sup>14</sup>CO<sub>2</sub>. We added an extra flask to the collection from June 2014.

Weekly sampling commenced in June 2014 and concluded in February 2016. To determine the

205 radiocarbon CO<sub>2</sub> content of our measurements, the samples are graphitized by INSTAAR and then sent for analysis to the accelerator mass spectrometer at the University of California at Irvine. Results are reported in  $\Delta^{14}\text{C}$  against the NBS Oxalic Acid I standard with an uncertainty of 1.8–2.5%. Over the course of the GAUGE project a total of around 250 samples were analysed for <sup>14</sup>CO<sub>2</sub>. From this analysis we also received information about the stable isotopes <sup>13</sup>CO<sub>2</sub>, CO<sup>18</sup>O, and <sup>13</sup>CH<sub>4</sub>, which

210 we do not report here. As part of the deployment of the Atmospheric Research Aircraft (described below) we collected glass flasks for the <sup>14</sup>CO<sub>2</sub> and Tedlar bags for analysis of <sup>13</sup>CH<sub>4</sub> by Royal Holloway, University of London. Using the aircraft allowed us to improve our knowledge of the spatial gradient of these gases. Samples were taken using an ORAC Metal bellows pump, fitted with



a pressure relief valve. For the glass flask sampling an adapter containing downstream pressure relief  
215 valve was used to prevent the accidental over pressurizing of the glass flasks during flight sampling.

A preliminary study of  $^{14}\text{CO}_2$  at Tacolneston during the GAUGE project has highlighted the  
benefits and difficulties associated with determining the fossil fuel content of  $\text{CO}_2$  in the UK. The  
key outcome from the measurement program has suggested that the amount  $\text{CO}_2$  originating from  
fossil fuel burning is not significantly different from model simulations using EDGAR emissions.  
220 However, there were a number of difficulties associated with making these measurements. First, we  
used a number of assumptions and data corrections to account for terrestrial biosphere fluxes and  
nuclear emissions. For nuclear emissions, we expect that the applied correction can be significantly  
improved by provision of higher frequency emissions data from the nuclear industry. Second, the  
location of the sampling site, timing and frequency of measurements is paramount in determining  
225 a strong enough  $^{14}\text{CO}_2$  signal from fossil fuels to distinguish it from the background uncertainty.  
Many lessons were learnt in the GAUGE project that will allow for an improved and more robust  
sampling strategy to be applied to future measurements (Wenger et al, "Atmospheric radiocarbon  
measurements to quantify  $\text{CO}_2$  emissions in the UK as part of the GAUGE project from 2014 to  
2015" in preparation for *Atmos. Chem. Phys. Discuss.*, 2018).

### 230 **East Anglian Church Network**

A key objective of GAUGE was to improve understanding how to attribute observed variations of  
GHGs to particular sectors. To help address that objective we established a regional network of five  
sensors over East Anglia (Figure 1, Table 4) where there is a high density of crop agriculture, a  
sector with large seasonal emissions of  $\text{CH}_4$  and  $\text{N}_2\text{O}$  attributed to fertilizer application (Section  
235 1). Developing this regional network supports the inference of higher resolution emission estimates  
(Manning et al., 2011). We used data from this network to determine how well we can distinguish  
between sources of  $\text{CH}_4$  from spatially diffuse agricultural sources to point sources such as landfills.

We purposely distributed the network across East Anglia (Figure 1), comprising one atmospheric  
observatory (Weybourne) and three churches (Holy Trinity, Haddenham; All Saints, Tilney; and St  
240 Nicholas, Glatton), and one wind turbine (Earl's Hall). East Anglia is one of several dense regions of  
UK agriculture. It was chosen for two reasons: 1) there is little variation in terrain height, simplifying  
boundary layer transport and mixing; and 2) all sites are within an hour of Cambridge, simplifying  
logistics associated with maintaining long-term sites. Additional criteria for site selection included  
sufficient sampling height (15–50 m for the East Anglia network, Table 4); remoteness from very  
245 local sources of  $\text{CH}_4$ ; easy accessibility for maintenance; and low running costs.

Figure 3 shows that the  $\text{CH}_4$  mole fraction data collected from the three churches exhibit similar  
variations on diurnal, daily, and monthly timescales, suggesting that either the surrounding villages  
have similar sources and/or at least some of the observed variation reflect larger-scale variations.  
Observed variations of  $\text{CH}_4$  at WAO are comparable to those at inland sites on seasonal timescales,





250 but are muted on faster timescales because it mainly observes clean upwind air. The shape of the diurnal cycle at the church sites suggests that the boundary layer likely plays the dominant role. Seasonal variations reflect changes in regional sources, boundary layer variations, and the OH sink.

Using the NAME-InTEM inverse model framework (Manning et al., 2011) we used the East Anglian network to infer county-level CH<sub>4</sub> fluxes for Cambridgeshire, Norfolk, and Suffolk. Our  
255 *a posteriori* fluxes were consistent with those from the UK National Atmospheric Emissions Inventory (Connors et al., “Estimates of regional methane emissions from inversion modelling – a proof of concept study,” in preparation for *Atmos. Chem. Phys. Discuss.*, 2018). For this work it was difficult to accurately estimate associated uncertainties because of difficulties associated with defining the ‘background’ CH<sub>4</sub> entering into the small, regional domain chosen. This difficulty will be avoided  
260 when these data are included in larger, regional-scale inversions. We find that regional networks, embedded within a nationwide network, show great potential for revealing additional spatial and temporal details of emissions such as point source emissions from landfills (Riddick et al., 2017). Such a regional network would best serve a national-scale network over regions where *a priori* emission uncertainties are largest.

## 265 2.2 Mobile GHG Measurement Platforms

We use mobile platforms to help integrate measurements that are sensitive to different spatial scales. The two principal platforms we use are the Rosyth-Zeebrugge North Sea ferry and the BAe-146 Atmospheric Research Aircraft. We also describe the deployment of balloon-borne sensors and a fixed-wing unmanned aerial vehicle (UAV), as examples of GAUGE fostering new atmospheric  
270 GHG measurement technology.

### North Sea Ferry

We installed an eight-foot air-conditioned sea container on the Rosyth (56.02262°N, 3.43913°W) to Zeebrugge (51.35454°N, 3.175863°E) ferry operated by DFDS Seaways. The container includes a Picarro 1301 CRDS to measure mole fractions of CH<sub>4</sub>, CO<sub>2</sub> and H<sub>2</sub>O. This ship of opportunity  
275 completes three return journeys per week traversing the North Sea at different times of day, thereby minimizing temporal measurement bias that can sometimes complicate the analysis of data from mobile platforms. The prevailing winds over the North Sea are westerly and southwesterly so that measurements frequently sample the outflow from the UK, and also allow us to distinguish between UK and mainland European emissions.

280 Figure 4 shows the view from the mobile laboratory, with sample inlets away from local sources on the ferry. The initial installation was on 25th February 2014 on DFDS Seaways Longstone (now the Finnmerchant) and ran until 15th April 2014. A weather station (Vaisala WXT 520) located on the top deck provides basic meteorological data (air temperature, pressure, wind speed and direction);



geo-location information (latitude, longitude, ship speed, course) is obtained from a Garmin GPS  
285 unit fixed to the roof of the sea container.

Figure 5 shows example CH<sub>4</sub> data for sailings in March, April, July, and September 2014, which  
shows a dynamic range that reflects geographical variations in sources. Differences between sailing  
reflect changes in seasonal emissions and prevailing meteorology. Figure 5 shows instances when  
observed values are influenced by emissions from the UK and the North Atlantic background during  
290 spring and summer (Figure 5a,b), and when observed values are influenced by high emissions from  
Germany and central Europe (Figure 5c) and by lower emissions from Scandinavia (Figure 5d). A  
more detailed description of the instruments and the data interpretation can be found in C. Helfter et  
al, “Temporal variability in country-scale greenhouse gas budgets using a mass balance approach,”  
in preparation for *Atmos. Chem. Phys. Discuss.*, 2018.

#### 295 **BAe-146 Atmospheric Research Aircraft**

We use the NERC/Met Office Atmospheric Research Aircraft (ARA), operated by AirTask Group  
Ltd, to provide vertical profile distributions of atmospheric GHGs over and around the British Isles.  
The specific objectives of deploying the ARA include: 1) collect a snapshot of precise and traceable  
GHG concentration distributions over and around the UK; 2) integrate atmospheric GHG informa-  
300 tion collected by tall towers, ferry transects, and space-borne instruments; 3) define and execute  
sampling experiments to enable measurement-led quantification of GHG fluxes at the regional scale  
( $\mathcal{O}(100\text{ km})$ ); and 4) define and execute sampling experiments to challenge Earth system models  
and flux inversion models in terms of better understanding model atmospheric transport error and  
surface emission distribution.

305 The ARA is a BAe-146-301 aircraft that has been converted to a mobile laboratory, including a  
variety of forward and backward facing external inlets so that air can be sampled by instruments  
within the main cabin. It also includes a number of ports that can host remote sensing instruments.  
Table 5 describes the instruments that we deployed during GAUGE, including in particular instru-  
ments that measure CO<sub>2</sub>, CH<sub>4</sub> and N<sub>2</sub>O, and a small complementary suite of other trace gases and  
310 thermodynamic parameters. We made continuous measurements of CO<sub>2</sub> and CH<sub>4</sub> at a frequency of  
1 Hz using a Fast Greenhouse Gas Analyser (FGGA, Los Gatos USA). For a detailed description of  
the FGGA, including its operating principles, data processing and calibration, we refer the reader to  
O’Shea et al. (2013). We also collect 1 Hz measurements of N<sub>2</sub>O and CH<sub>4</sub> from a quantum cascade  
laser absorption spectrometer (Aerodyne Research Inc., USA). Further details of the instrument are  
315 described by Pitt et al. (2016). We use the Met Office Airborne Research Interferometer Evaluation  
System (ARIES), a Fourier transform infrared spectrometer, to retrieve partial columns of CH<sub>4</sub> and  
CO<sub>2</sub> and vertical profiles of H<sub>2</sub>O and temperature. Further details about ARIES can be found in  
Allen et al. (2014). Other instruments listed in Table 5 are core ARA science instruments, which are  
described in Allen et al. (2011) and references therein.



320 During GAUGE we conducted a total of 16 individual flight sorties over/around mainland UK  
and Ireland between May 2014 and March 2016, comprising over 65 hours of atmospheric sam-  
pling. These flights are summarized in Table 6 and Figure 6. A typical flight sortie coordinated  
upwind and downwind sampling of a target flux region (e.g., the London metropolitan area), based  
on the prevailing boundary layer wind direction, to attempt sampling of airmasses that have been im-  
325 pacted by regions with GHG emissions and uptake. We also designed flights to sample outflow from  
mainland UK and continental Europe, and outflow from the Irish and North seas on days with strong  
westerly flow regimes, e.g. J. Pitt et al, “Development of a method to assess CH<sub>4</sub> flux using aircraft  
and ground-based sampling: a case study for the British Isles on 12 May 2015,” in preparation for  
*Atmos. Chem. Phys. Discuss.*, 2018.

330 To capture regional emissions during GAUGE, we collected measurements that were mostly in  
the boundary layer, as defined by in-flight thermodynamic profiling, which was typically below  
2 km altitude. Occasionally, to characterize long-range transport of pollutants into our study region,  
we collected measurements during deeper vertical profiles into the free and upper troposphere. Other  
flight profiles included surveys around Britain and Ireland and flying around tall towers, as described  
335 below.

Figure 6 shows a summary plot of the CO<sub>2</sub> and CH<sub>4</sub> data collected during GAUGE. In particular,  
it illustrates the horizontal and vertical spatial coverage of the aircraft sampling, and the dynamic  
range of mole fractions sampled. These observed variations are due to differences in flight altitude  
and the time of year of the superimposed flights (Table 6), differences in airmass history, and the  
340 spatial and temporal variability of local and regional fluxes across seasons and sources.

Table 7 shows a comparison between aircraft and tall tower data during aircraft fly-pasts. The  
mean difference between CO<sub>2</sub> (CH<sub>4</sub>) observations at all tall tower sites measured during 12 individ-  
ual flights is  $0.72 \pm 1.69$  ppm ( $-1.22 \pm 12.54$  ppb). Taking into account that the majority of the flights  
took place during summer months, the magnitude of these difference is as expected with generally  
345 lower CO<sub>2</sub> and higher CH<sub>4</sub> mole fractions closer to the ground and more sensitive to local fluxes.

### Balloon CO<sub>2</sub> Sondes

Balloons offer an alternative platform for the collection of vertical profiles of GHGs, building on  
the approaches used widely by the meteorological and stratospheric communities. Here, we describe  
some of the first balloon launches of small-scale CO<sub>2</sub> sensor technology that have been adapted for  
350 atmospheric sciences. ChemSonde is a balloon-based instrument, developed as part of a collabora-  
tion between the University of Cambridge, SenseAir (Sweden), with additional input from Vaisala  
(Finland) and Alphasense (UK). The aim of ChemSonde is to provide a cheap method for measuring  
CO<sub>2</sub> concentrations from the surface to  $\approx 30$  km on a global scale by using the existing radiosonde  
infrastructure, and to form the basis of a calibration/validation programme to support space-borne  
355 observations of GHGs.



The instrument consists of a small, sensitive nondispersive infrared CO<sub>2</sub> sensor developed by SenseAir, Sweden, ([www.senseair.se](http://www.senseair.se)) which has been adapted for atmospheric measurements. The instrument sampling is 1 Hz with data transmitted to the Vaisala MW41 ground station via the radiosonde. The corresponding vertical resolution of the collected data is 4–5 m. The dimensions and weight of the instrument package are approximately 150×150×300 mm and 1 kg, respectively. Heavy-duty cable ties are used to seal the enclosure and secure the radiosonde to the outside. A 1200 g balloon (TOTEX, Japan) is used for lifting the payload.

Figure 7 shows preliminary data from two ChemSonde launches from WAO on the 14th April 2016 to test the viability of the system. Met Office surface analysis charts (not shown) indicate that the UK was under the influence of a low pressure anticyclone in the North-Atlantic, transporting moist air over the southern half of the UK, during the period of measurements. A low-level stratus cloud deck, with drizzle, and low SW winds predominated over WAO during the morning of the 14th April, with light winds and steady rain during the afternoon. The first instrument was launched at 1039 UTC, and the second at 1430 UTC. For brevity, we only show data to 10 km. The sharp decrease in CO<sub>2</sub> from near-surface altitudes to  $\approx 1$  km during the morning launch, and the increase in boundary-layer CO<sub>2</sub> concentrations from morning to afternoon launches suggest some local influence. We also noticed that some small-scale increases in CO<sub>2</sub> (1.8 km and 7.5 km from the morning launch and 2.5 km from the afternoon launch) correspond to increased relative humidity, indicating possible cloud layers. NOAA HYSPLIT 48-hour back trajectories (Stein et al., 2015) initialized at these lower and mid troposphere altitudes (not shown) indicate that we are sampling background maritime air over the North Atlantic that has been lofted prior to interaction with land surfaces. Differences in relative humidity close to 6 km suggest that the morning cloud structure has been dissipated by the stronger afternoon winds. We attribute the 4–5 ppm difference between CO<sub>2</sub> instruments above 6.5 km to problems with the zero baseline drift, and to a faulty span measurement during the afternoon pre-launch preparation. Further studies with ChemSonde are planned, with emphasis on improving design, operation and the post-processing of data.

### Unmanned Aerial Vehicles for Hotspot Measurement Campaign

UAVs represent a new atmospheric measurement platform for studying atmospheric GHGs. They can be deployed rapidly to provide vertical information across a horizontal dimension  $\mathcal{O}(100$  m). Within GAUGE, researchers used a variety of measurement technologies, including fixed-wing and rotary UAVs, to develop and refine new methods to use atmospheric measurements to quantify CH<sub>4</sub> and CO<sub>2</sub> emission from a landfill site (Riddick et al., 2016; Sonderfeld et al., 2017; Allen et al., 2017; Riddick et al., 2017). This represents one of the first demonstrations of using UAVs to sample GHG emissions. The reader is referred to Allen (2014); Allen et al. (2015) for further details of the underlying technology.



We conducted a two-week measurement campaign at a landfill site near Ipswich, England (operated by Viridor Ltd) in August 2014. This campaign brought together researchers from Universities of Bristol, Cambridge, Denmark Technical University, Edinburgh, Leicester, Manchester, Royal Holloway University of London, Southampton, and Ground Gas Solutions (GGS) Ltd. The landfill  
395 includes historic, capped and active, open landfill cells, a leachate plant, a gas collection network and gas burning energy generation facility.

We equipped the site with a 20 m eddy covariance flux tower, three Los Gatos Research ultra-portable greenhouse gas ( $\text{CO}_2$  and  $\text{CH}_4$ ) analysers (triangulated across the capped and open cell areas), a closed path FTIR, and five 3-D sonic anemometers to characterize flow over the site. Con-  
400 ventional walkover flux surveys were conducted by GGS and dynamic automated flux chambers were operated on the flanks of the capped landfill area to investigate seeps under the capped area where this met an active cell. Tracer releases of perfluorocarbon and acetylene were also conducted from various key points across the site to allow proxy flux calculations from mobile (public road) plume sampling downwind. Specific experiments and instrument-siting were designed on each day  
405 of the intensive period in response to weather (especially wind) conditions to characterise inflow and outflow from different areas of the site. We deployed a fixed-wing UAV equipped with a  $\text{CO}_2$  sensor around the site. We also launched a tethered rotary UAV, which sampled air up to 120 m above the local terrain and analyzed using ground-based instruments via a 150 m length of Teflon tube. This configuration allowed us to sample vertical profiles of  $\text{CH}_4$  and  $\text{CO}_2$  over the landfill site.

We also established a fixed-site monitoring station measuring  $\text{CO}_2$  and  $\text{CH}_4$  mole fractions to put  
410 the campaign into a longer temporal context, to help test plume inversion techniques, and to test the efficacy of continuous *in situ* monitoring to generate flux climatologies (Riddick et al., 2016, 2017). Sonderfeld et al. (2017) demonstrate how to combine computational fluid dynamics model (which accounts for topographical data from a 3-D LiDAR survey data) with continuous *in situ* FTIR  
415 measurements to infer and apportion fluxes across the surface area of the landfill site. They showed in particular the ability of this approach to distinguish between individual emission regions within a landfill site, allowing better source apportionment compared with other methods that derive bulk emissions.

Our UAV deployment during this experiment has since led to further refinements to the method  
420 and platform, and to our use of similar technology to infer fluxes from other UK landfills (Allen et al., 2017). A recent validation of a new mass balancing algorithm based on UAV sampling of a known  $\text{CH}_4$  release rate demonstrated that a 20-minute flight on a single rotary UAV flight can reproduce the known release rate with an mean accuracy of 14% and an ( $1\sigma$ ) uncertainty of <40% (Shah et al., 2017). Collectively, these measurements allowed us to test and compare a wide range of  
425 established and novel sampling technologies and flux quantification approaches. It also allowed us to examine how to optimize different combinations of data to determine net bulk (whole-site) GHG fluxes.



### 2.3 Space-borne Observations of GHGs

Satellites provide global, near-continuous and multi-year measurements of GHGs that are used to  
430 infer GHG fluxes on sub-continental scales, and to provide boundary conditions for regional at-  
mospheric transport models. Within GAUGE, we explore the potential of short-wave IR (SWIR)  
column measurements of CO<sub>2</sub> and CH<sub>4</sub> from the Japanese Greenhouse Gases Observing SATellite  
(GOSAT) and thermal IR column measurements of CH<sub>4</sub> from the European Infrared Atmospheric  
Sounding Interferometer (IASI). For the sake of brevity, we describe here only the pertinent details  
435 of GOSAT and IASI and refer the reader to other studies dedicated to these satellite instruments (e.g.  
Kuze et al. (2009); Clerbaux et al. (2009)).

GOSAT is the first space-borne mission dedicated to measuring GHGs. It was launched in a sun-  
synchronous orbit with a local overpass time of 1300 by the Japanese Space Agency (JAXA) in  
January 2009 (Kuze et al., 2009). We use the Thermal And Near-infrared Sensor for carbon Observa-  
440 tion (TANSO) FTS that observes atmospheric spectra and the Cloud and Aerosol Imager (CAI) that  
provides multi-spectral imagery and coincident cloud and aerosol information (Kuze et al., 2009).  
TANSO-FTS has a ground footprint of approximately 10.5 km<sup>2</sup> and returns to the same point every  
three days. For illustration, we show GOSAT SWIR dry-air column-averaged CH<sub>4</sub> mole fractions  
that are inferred from version 7.0 of the proxy retrieval developed by the University of Leicester  
445 (section 3). These data are sensitive to changes in atmospheric CH<sub>4</sub> in the lower troposphere. The  
proxy retrieval method simultaneously fits CH<sub>4</sub> and CO<sub>2</sub> spectral features in nearby wavelengths.  
The underlying idea is that taking the ratio of the CH<sub>4</sub> and CO<sub>2</sub> fitted in nearby wavelength regions  
effectively removes spectral artefacts common to both CH<sub>4</sub> and CO<sub>2</sub> (e.g., scattering). The conven-  
tional method of using these data is to multiply the ratio by model CO<sub>2</sub>, assuming that CO<sub>2</sub> varies in  
450 space and time less than CH<sub>4</sub>. The resulting proxy XCH<sub>4</sub> data have been evaluated extensively using  
data from the Total Carbon Observing Network (Parker et al., 2011, 2015).

IASI is one of a series of Fourier Transform Spectrometer (FTS) instruments on the polar-orbiting  
meteorological MetOp platforms (Hilton et al, 2012) designed primarily for operational meteorol-  
ogy. There are two IASI instruments currently operating: MetOp-A was launched on 19th October  
455 2006 and MetOp-B was launched on 17th September 2012. IASI has an across-track measurement  
swath of 2,200 km, resulting in near-global coverage twice a day with a local solar overpass time  
of 0930 and 2130. It measures three spectral bands that span a range of thermal IR wavelengths  
from 4 microns to 15.5 microns (Clerbaux et al., 2009), which are most sensitive to CH<sub>4</sub> in the mid-  
troposphere. Vertical profile retrievals of column-averaged volume mixing ratios of atmospheric CH<sub>4</sub>  
460 have been inferred using optimal estimation from IASI spectra by the Rutherford Appleton Labora-  
tory (Siddans et al., 2017). The retrieval produces two pieces of information in the mid/upper tro-  
posphere each with a single retrieval precision of 20–40 ppbv. Differences between IASI and GOSAT  
CH<sub>4</sub> are within 10 ppbv except over southern mid-latitudes where IASI is lower than GOSAT by  
20–40 ppbv (Siddans et al., 2017).



465 The spatial coverage of satellite SWIR observations of CO<sub>2</sub> and CH<sub>4</sub> over the UK is limited  
mainly by cloud-free scenes that are themselves determined by the spatial resolution of the instru-  
ments and the repeat frequency of the orbits. Currently, there are insufficient cloud-free data to  
overtake the information provided by the *in situ* measurements. However, we will soon have daily  
CH<sub>4</sub> measurements from TROPOMI aboard Sentinel-5P, launched 16th October 2017. Data from  
470 future and planned missions represent at least an order of magnitude more satellite data than we  
have now. Until then, these data GOSAT represents constraints on larger-scale sub-continental CO<sub>2</sub>  
and CH<sub>4</sub> flux estimates (e.g. Feng et al. (2017)).

#### 2.4 Intercalibration activities

Linking measurements in the GAUGE network to a common calibration scale ensures compara-  
475 bility of these measurements, and simultaneously linking them to a common set of traceable gas  
standards ensures they are also compatible with ongoing international GHG measurement activities.  
Two prominent examples of such activities include the pan-European Integrated Carbon Observing  
System (ICOS, <https://www.icos-ri.eu/>) and the Integrated Global Greenhouse Gas Information Sys-  
tem (IG<sup>3</sup>IS, <https://goo.gl/4t1x6i>). The GAUGE project encompassed a large number of data streams  
480 collected using a range of instrumental techniques and at a variety of temporal resolutions, increas-  
ing the risk of compatibility and comparability errors. Inversion methods used in GAUGE to infer  
GHG fluxes from atmospheric mole fraction measurements are particularly sensitive to site biases  
and offsets (Law et al., 2008). Consequently, ensuring comparability and assessing compatibility  
was key to the success of GAUGE.

485 As far as possible we ensured measurement comparability by linking all observations directly to  
common WMO calibration scales, but due to the historical nature of some data records this was not  
uniformly possible. All CO<sub>2</sub> measurements collected within the project were linked to the WMO  
x2007 scale. All CH<sub>4</sub> measurements, other than MHD GC-FID (Table 2) that uses the Tohoku scale,  
were calibrated to the WMO x2004A scale. In contrast, N<sub>2</sub>O measurements used either the SIO-98  
490 scale (MHD and the rural tall tower sites BSD, HFD, RGL, TAC and TTA) or the WMO x2006A  
scale (all other locations).

### 3 Numerical Models of Atmospheric GHGs

Figure 8 shows the modelling strategy we employed to quantify the magnitude, distribution and un-  
certainty of UK emissions of GHGs from different sectors. We use models of atmospheric chemistry  
495 and transport, using prescribed *a priori* flux estimates, to describe the relationship between sector  
emissions of GHGs and atmospheric variations observed by the fixed and mobile GHG measurement  
platforms used during GAUGE (Figure 1). These models, which account for instrument-specific  
sampling, constitute the forward model. Inverse models infer the magnitude and uncertainty of re-



gional flux estimates by fitting the forward model to observations, accounting for their respective  
500 uncertainties.

Because of the complex physical and chemical relationships between the surface fluxes and the atmospheric observations, and because of the assumptions embedded within individual models, we use a range of atmospheric transport models and inverse methods to mitigate criticism that our results depend only one model.

### 505 3.1 Atmospheric Chemistry Transport Models

Table 9 summarizes the three different chemical transport models (CTMs) and one atmospheric dispersion model that we use to interpret the GAUGE data. All models are well established and have been used to interpret a wide range of atmospheric GHG measurements.

#### Brief Description of Individual Models

510 We use the following models: 1) the Goddard Earth Observing System atmospheric Chemistry transport model (GEOS-Chem) (Feng et al., 2011; Fraser et al., 2013; Deng et al., 2014; Feng et al., 2017); 2) the Model for Ozone and Related chemical Tracers (MOZART) (Emmons et al., 2010); 3) the TOMCAT model (Wilson et al., 2016; McNorton et al., 2016; Monks et al., 2017); and 4) the Numerical Atmospheric dispersion Modelling Environment (NAME) (Jones et al., 2007). These models  
515 vary in their basic methodologies for representing atmospheric transport, parameterisations of physical atmospheric processes, and in their horizontal and vertical resolutions. We have ensured, as much as possible, that we use common model boundary conditions (e.g., flux inventories and lateral boundary conditions for regional models). Model differences therefore provide us an opportunity to quantify the impact of model error on describing observations and consequently on inferred GHG  
520 flux estimates. For further details about an individual model, the reader is encouraged to consult the model-specific literature as provided above.

For the purpose of this overview of GAUGE and as part of our model assessment within GAUGE, we ran global 3-D experiments to describe observed variations of CO<sub>2</sub>, CH<sub>4</sub> and N<sub>2</sub>O from 2004 to 2016, including the main GAUGE measurement period of 2014–2015, inclusively. The CTMs used  
525 common flux estimates and chemical loss fields as described below. Preparation of these estimates, collected from different sources, were regridded to the different model resolutions (Table 9), ensuring that the total emitted mass was conserved. The CTMs also used common atmospheric mole fraction initial conditions for 2003.

To describe anthropogenic emissions of CO<sub>2</sub> from 2003 to 2009, we use the Carbon Dioxide Information Analysis Center (CDIAC) inventory (available online at <http://cdiac.ornl.gov/trends/emis/overview.html>).  
530 In later years, we repeat values from 2009. We use the NASA-CASA biosphere model (Olsen and Randerson, 2004) to describe terrestrial biospheric fluxes, 2003–2015, including biomass burning





emissions. Climatological ocean fluxes of CO<sub>2</sub> are taken from Takahashi et al. (2009), covering the period 2003–2011.

535 The formulation of our CH<sub>4</sub> simulations generally follows Wilson et al. (2016); McNorton et al. (2016). We use updated anthropogenic CH<sub>4</sub> emissions from the Emission Database for Global Atmospheric Research (EDGAR) v4.2FT inventory Olivier et al. (2012), covering the period 2000–2010. We repeat 2010 emissions for years beyond 2010. Biomass burning emissions were taken from the Global Fire Emissions Database (GFED) v3.1 inventory (van der Werf et al., 2010). Wetland and  
540 rice emissions were taken from Bloom et al. (2012). Other natural emissions, including the soil sink (treated as a negative flux) were taken from the TransCom CH<sub>4</sub> model intercomparison (Patra et al., 2011). We use monthly 3-D mean OH fields taken from Patra et al. (2011) to describe the main atmospheric sink of CH<sub>4</sub>. Reaction rates are taken from Sander et al. (2006). Stratospheric loss of CH<sub>4</sub> due to reaction with O(<sup>1</sup>D) and Cl radicals are based on loss rates taken from the Cambridge 2-D  
545 model (Velders, 1995). The resulting atmospheric lifetime of CH<sub>4</sub> is  $\simeq 10$  years, which is determined mainly by the tropospheric OH sink.

Fluxes for our N<sub>2</sub>O simulations are taken from four broadly defined source categories: natural soils (Saikawa et al., 2014), agricultural and other anthropogenic emissions (Olivier et al., 2012), ocean fluxes (Manizza et al., 2012), and biomass burning (van der Werf et al., 2010). We parameterized an offline stratospheric loss of N<sub>2</sub>O in each model using photolysis and O(<sup>1</sup>D) climatologies  
550 (Thompson et al., 2014). We did not consider this sink for NAME because of the short duration of model runs compared to the atmospheric lifetime of N<sub>2</sub>O ( $\simeq 120$  years). The relatively long atmospheric lifetime of N<sub>2</sub>O, determined by stratospheric sinks, means that interpreting observed tropospheric variations of N<sub>2</sub>O presents different challenges to interpreting observed variations of  
555 CH<sub>4</sub>.

#### Assessment of Model Performance using Large-scale Independent data

To assess the global-scale GAUGE models we use data that are representative of large spatial and temporal scales. In particular, we use surface mole fraction data from NOAA/ESRL and column data from the GOSAT and IASI satellite instruments (Section 2). We use these data to evaluate the  
560 three free-running CTMs, described above, by sampling each model at the time and location of each observation.

Figure 9 shows that the models reproduce the broad scale zonal-mean distribution of CO<sub>2</sub> and CH<sub>4</sub>. Given the common set of source and sink terms, model divergence will mostly reflect differences in atmospheric transport. Generally, the largest model biases for CO<sub>2</sub> are at mid/high northern  
565 latitudes where the emissions are largest. Model divergence is highest at these latitudes during northern winter months, with GEOS-Chem having the largest model bias during these months. Model performance generally improves in the northern summer months with model differences typically within a few ppm and much closer to the observations. The model spread supports our strategy of



using different models to infer GHG fluxes. For CH<sub>4</sub>, the models have a similar level of skill. None  
570 of the models reproduce the observed inter-hemispheric gradients, likely due to errors in the *a priori*  
distribution of emissions used by the inventories. The model spread is largest in January with a value  
of 45 ppb. Model performance for N<sub>2</sub>O is the most variable, although this partly reflects that N<sub>2</sub>O has  
the smallest observed inter-hemispheric gradients of the three gases. The maximum model range is  
1.4 ppb and 1.7 ppb in January and July, respectively. The GEOS-Chem and MOZART models have  
575 gradients similarly small in the southern hemisphere and tropics, while TOMCAT is much larger.

Figure 10 shows that MOZART and GEOS-Chem have similar vertical distributions of CH<sub>4</sub> dur-  
ing July, displaying a stronger vertical gradient from the surface to 400 hPa than the TOMCAT  
model. This corresponds to higher northern hemispheric mole fraction values. During July, the three  
models all display different rates of vertical transport throughout the northern hemisphere tropo-  
580 sphere. TOMCAT has a slight gradient between the surface and 600 hPa, and a much steeper gradient  
above; MOZART displays the opposite behaviour; and GEOS-Chem lies between those extremes.  
Differences in atmospheric transport are important and for some gases can represent a substantial  
fraction of the signal. Our use of multiple models and combining the resulting analysis improves our  
ability to quantify the uncertainty of our results.

585 We also evaluate the models using the GOSAT Proxy XCH<sub>4</sub> V7.0 data product developed by  
the University of Leicester (<http://www.esa-ghg-cci.org/>) and the IASI MetOp-A thermal IR V1.0  
XCH<sub>4</sub> data products developed by the Rutherford Appleton Laboratory (<http://dx.doi.org/10.5285/B6A84C73-89F3-48EC-AEE3-592FEF634E9B>).

Figure 11 shows the spatial coverage provided by both instruments during June–August 2014.  
590 The sparser coverage of GOSAT observations reflects its sensitivity to clouds and aerosols. Mea-  
surements over the ocean used a glint observing model that takes advantage of specular reflection  
and its associated high signal to noise ratio. Despite GOSAT and IASI observing different parts of  
the atmosphere there are many common features associated with fossil fuel extraction/combustion  
(North America, China, and parts of Saudi Arabia), wetlands (South America, Africa, and part of  
595 India and China), and rice paddies (mostly India and China). Both GEOS-Chem and TOMCAT  
model reproduce the broad spatial distributions of GOSAT and IASI CH<sub>4</sub> observations (not shown),  
with negative global mean model biases that are approximately 10 ppb for GOSAT and between  
1 ppb (GEOS-Chem) and 10 ppb (TOMCAT) for IASI. These biases mainly reflect errors in *a priori*  
surface emissions, but also errors in modelling stratospheric CH<sub>4</sub> (e.g. Alexe et al. (2015)).

### 600 3.2 Inverse Methods

The ultimate objective of GAUGE is to characterize the magnitude, distribution, and uncertainty of  
UK GHG emissions. Relating *a priori* GHG flux estimates to the atmosphere sampled at the time and  
location of observations is called the forward problem (Figure 8). The corresponding inverse problem  
refers to the process of relating observed atmospheric measurements to the underlying geographical



605 distribution of GHG fluxes. Each of the atmospheric transport models listed above employ their own  
inverse method, as described below.

Inferring CO<sub>2</sub>, CH<sub>4</sub>, and N<sub>2</sub>O fluxes directly from atmospheric observations is generally an ill-  
posed inverse problem, with a wide range of scenarios that could fit these data. *A priori* information  
is used to regularize the problem (Figure 8).

610 The results of inverse modelling are typically dependent on the distribution of the observations  
used. For example, the sparsity of data at low latitudes places a limit on our ability to infer GHG  
fluxes over geographical regions that are not well sampled, e.g. tropical ecosystems. The spatial and  
temporal density of GHG measurements collected during GAUGE allows us to constrain *a posteriori*  
emission estimates on devolved UK administration scale and on sub-annual timescales.

615 Although Bayes' theorem provides the basis for each of the inverse modelling techniques used in  
GAUGE, each approach employs a slightly different methodology to infer optimized surface fluxes.  
As we have already seen there can be relatively large differences in atmospheric transport models.  
Indeed, the errors associated with atmospheric transport models are typically the largest source of  
error in estimating GHG fluxes.

620 In the interest of brevity, we only briefly introduce the inverse methods employed within GAUGE  
and refer the reader to dedicated cited papers on the techniques.

The global and nested GEOS-Chem model is linked with an ensemble Kalman filter (Feng et al.,  
2009, 2011, 2017). This approach does not require that we linearize the model but assumes approxi-  
mate Gaussian statistics. The ensemble Kalman filter approach allows us to include easily estimates  
625 of model atmospheric transport error. Flux estimates are resolved on geographical regions informed  
by the ability of the data to independently estimate fluxes on those spatial scales. Over the UK,  
fluxes are estimated on pre-defined aggregated county levels and on a weekly scale. Weekly values  
are subsequently aggregated to longer timescales to minimize autocorrelation between successive  
flux estimates.

630 The inverse version of the TOMCAT model, INVICAT (Wilson et al., 2014) uses a variational  
inversion method based on 4D-Var. This approach uses the adjoint version of the forward model to  
minimize the *a posteriori* fit between the model and data. This is an iterative method that can some-  
times require a large number of iterations before convergence. Consequently, we resolve *a posteriori*  
emissions using TOMCAT at a spatial resolution of 2.8°.

635 The NAME model uses the InTEM inverse method, building on Manning et al. (2011) but now  
posed in a hierarchical Bayesian method in which the basis function decomposition of the flux space,  
and the model and *a priori* uncertainties, are explored using reversible-jump MCMC (Ganesan et al.,  
2014; Lunt et al., 2016). For the MOZART model we used a hierarchical Bayesian method based on  
Ganesan et al. (2014). InTEM estimates emissions across a north west European domain at horizontal  
640 resolutions from 25 km to 100s km, depending on the frequency of sampling different regions.  
Boundary conditions are solved within each NAME inversion, following Ganesan et al. (2015) for



InTEM and Lunt et al. (2016) for the MCMC approach. Monthly UK emission estimates of CH<sub>4</sub> and N<sub>2</sub>O were estimated for the period 2013–2016 and compared to the reported inventory.

Our GAUGE inverse model studies generally include a series of factorial experiments that allowed  
645 us to explore the relative importance of individual and collective data to estimate UK CO<sub>2</sub> and CH<sub>4</sub>  
flux estimates. Based on these experiments we define a control experiment. We test the robustness of  
our results by comparing results from using half/double assumed measurements uncertainties. UK  
*a posteriori* flux estimates for CO<sub>2</sub> and CH<sub>4</sub> are currently being prepared for publication: Lunt et al,  
“Evaluating national methane emissions using atmospheric observations,” in preparation for *Atmos.*  
650 *Chem. Phys. Discuss.*, 2018. and Palmer et al, “Using atmospheric measurements to verify UK net  
fluxes of carbon dioxide,” in preparation for *Atmos. Chem. Phys. Discuss.*, 2018. Broadly speaking,  
we have estimated net CO<sub>2</sub> fluxes using regional and global-scales, but have been unable to attribute  
those fluxes to specific sectors; for CH<sub>4</sub>, using the continental-scale data and the regional network  
data, we have begun to improve our understanding of sector emissions; and for N<sub>2</sub>O, which has the  
655 small atmospheric gradients due to its long atmospheric lifetime, we have not begun to analyze the  
data collected within GAUGE.

#### 4 Concluding Remarks

The main objective of the Greenhouse gAs Uk and Global Emissions (GAUGE) project was to esti-  
mate the magnitude, distribution, and uncertainty of UK emissions of three atmospheric greenhouse  
660 gases (GHGs): carbon dioxide (CO<sub>2</sub>), methane (CH<sub>4</sub>), and nitrous oxide (N<sub>2</sub>O). To achieve that ob-  
jective, we established an inter-linked measurement and data analysis programme of activities from  
2013 to 2015. These activities substantially expanded on existing measurements and data analysis.  
Some measurements that were established as part of GAUGE have continued beyond 2015. The  
primary motivation for GAUGE was to develop a measurement-led system to verify UK GHG emis-  
665 sions in accordance with the UK Climate Change Act 2008. GAUGE also lays the foundations for  
estimating nationally determined contributions as part of the Paris Agreement.

Emissions of CO<sub>2</sub>, CH<sub>4</sub>, and N<sub>2</sub>O represented 97% of UK GHG emissions during 2015 (the latest  
budget estimates available from the UK government). These emissions originate from a variety of  
sectors, including energy supply, transport, business, residential, agriculture, waste management, and  
670 other. These emissions are very different in nature, ranging from point sources to large-scale, diffuse  
sources. We considered this heterogeneity of course when we designed the GAUGE measurement  
programme.

The backbone of GAUGE is a network of measurements that are collected at height from telecom-  
munication masts, tall towers, distributed across the UK. These measurements are typically collected  
675 at multiple inlet heights (100–300 m) above the local terrain (and sources) so they have a reasonable  
fetch suitable for quantifying sub-national scale GHG fluxes. GAUGE added two tall tower sites



to the UK Deriving Emissions linked to Climate Change (DECC) tall tower network. The DECC network was established in 2012 to estimate GHG emissions from the UK devolved administrations. The GAUGE sites included a site on the North Yorkshire Moors, with sensitivity to the Greater  
680 Manchester-Leeds-Liverpool-Sheffield region, and in East Sussex that has sensitivity to emissions from London.

We collected data on a commercial ferry that travelled regularly between Rosyth, Scotland, and Zeebrugge, Belgium. This mobile measurement platform provided information on UK and mainland European outflow of GHGs, which complemented the tall tower data. Using a regional tower net-  
685 work over East Anglia, comprising mostly of measurements collected on Church steeples, we found additional spatial and temporal flux distributions over the region could be achieved. We chose East Anglia because it is where there is a high density of agriculture, and where the local terrain is relatively flat so that church steeples often represent the highest local landmarks. As part of GAUGE we deployed the UK Atmospheric Research Aircraft for a limited number of flights around and across  
690 the UK. These data have been used to study the transport of atmospheric GHGs on local to regional spatial scales.

To explore how the UK GHG measurement network could develop in the future, we incorporated new technologies and new measurement platforms into the GAUGE programme. We deployed small sensors that were launched on a small number of sonde launches, which offer a potentially new  
695 way to obtain vertical distributions of GHGs. We also used unmanned aerial vehicles as part of a larger measurement campaign to characterize GHG emissions from a landfill, helping to pave the way for using this technology more generally within larger-scale GHG emission experiments. We also explored how we can use satellites effectively to estimate UK GHG fluxes. The spatial and temporal coverage of clear-sky measurements over the UK from current SWIR instruments, which  
700 are sensitive to changes  $\text{CO}_2$  and  $\text{CH}_4$ , are too sparse to provide competitive constraints on  $\text{CO}_2$  fluxes. We anticipate this situation will slowly change with new instruments (e.g. TROPOMI) and proposed mission concepts (e.g. Copernicus  $\text{CO}_2$  service) that will result in higher spatial resolution and consequently more cloud-free scenes.

We used a range of global and regional atmospheric transport models linked with inverse methods  
705 to interpret the atmospheric GHG observations. We showed that these models have skill in reproducing observed atmospheric  $\text{CO}_2$  and  $\text{CH}_4$  variations on hemispheric scales, but disagree with  $\text{N}_2\text{O}$  observation due to much small gradients that reflect its longer atmospheric lifetime. This multi-model approach was adopted to help study the model spread in *a posteriori* GHG fluxes, and to study the relative importance of individual data to estimate UK GHG fluxes. For this work, we refer  
710 the reader to the dedicated papers.

We approached source attribution in two ways. First, we used the regional-scale network to improve the distribution of  $\text{CH}_4$  fluxes due to agriculture, taking advantage of reasonable spatial disaggregation of this source over East Anglia. We also established an isotope measurement programme,



including concurrent measurements collected at Mace Head, Ireland, and Tacolneston, East Anglia.  
715 Data from these two sites provided a crude meridional gradient over the UK. Our sampling approach  
was designed, using the prevailing wind direction over the UK, to determine the gradient due to  
fossil fuel CO<sub>2</sub>. Despite our best efforts, neither approach to source attribution was definitive. For  
example, our analysis of radiocarbon was compromised by the influence of the nuclear power sec-  
tor. We anticipate the development a more optimal sampling approach is possible by working more  
720 closely with this sector to avoid instances when sampled air masses are dominated by upwind the  
nuclear source.

GAUGE represents a first concerted attempt by the UK science community to quantify nation-  
wide GHG fluxes. We have laid the foundations of measurement infrastructure that moves forward  
with a better understanding of the advantages and disadvantages of individual GHG data. The post-  
725 GAUGE tall tower network has continued. For instance, the UK DECC network has adopted North  
Yorkshire site, which provides valuable flux information about northern England and to a lesser ex-  
tent southern Scotland, and the National Physical Laboratory now runs the tall tower at Heathfield.  
We also anticipate a growing role for satellite observations, which are free at the point of delivery, as  
new instruments provide better spatial coverage and probabilistically a higher number of cloud-free  
730 scenes. Data analysis will continue as improved models and inverse methods progressively better  
describe the physical and chemical processes that determined atmospheric GHGs. The UK is a ge-  
ographically small country and plays a proportional role in the Paris Agreement, but we expect the  
design of GAUGE can be scaled upwards to larger geographical regions, taking advantage of specific  
technologies relevant to the sectors that dominate continental GHG budgets.

735 *Acknowledgements.* The GAUGE project was funded by the Natural Environment Research Council under  
grant reference NE/K002449/1. We gratefully acknowledge the cooperation and efforts of the station operators  
Gerard Spain and Duncan Brown at Mace Head monitoring station, and Stephen Humphreys at the Tacolneston  
tall tower station. We also thank the Physics Department, National University of Ireland, Galway, for making  
available the research facilities at Mace Head. We thank the Parish councils of Holy Trinity, Haddenham, Cam-  
740 bridgeshire; All Saints, Tilney St Lawrence, Norfolk; and St Nicholas, Glatton, Cambridgeshire as well as  
Greencoat Capital for their kindness and assistance in hosting instruments in our East Anglian network. The  
Diocese of Ely was instrumental in facilitating their involvement, and we especially acknowledge the assistance  
of Bill Murrells, David Ogilvie, and the Revs Fiona Brampton, Nigel Cooper, Martin Dale, Barbara Pearman  
and Rosie Ward. We thank collaborators at the Universities of Southampton, Royal Holloway University Lon-  
745 don, and Ground Gas Solutions Ltd for their support of the landfill case study, and Viridor Ltd for providing  
on-site support and facilitated access to their operational site; staff (including pilots) at the Facility for Air-  
borne Atmospheric Measurement, Airtask Ltd, and Avalon Engineering Ltd for their support in conducting  
airborne fieldwork; DFDS Seaways for authorising the research activities on board the Rosyth-Zeebrugge com-  
mercial ferry; Captains and crews of the Longstone (now the Finnmerchant) and Finlandia Seaways for access  
750 to the ships and for supporting the day-to-day research operations; Ray Freshwater and Bin Ouyang (Chemistry



Department, University of Cambridge) for invaluable technical assistance and design of the ChemSonde motherboard, and for processing the ChemSonde raw CO<sub>2</sub> data; and Grant Forster (University of East Anglia) for access and assistance at NCAS-funded Weybourne Atmospheric Observatory. L. F. also acknowledges funding from the NERC National Centre for Earth Observation. P.I.P. gratefully acknowledges his Royal Society  
755 Wolfson Research Merit Award. J.P. and S.C. were funded by NERC PhD studentships NE/L501/591/1 and NE/J500070/1, respectively. N.H. also received support from Defra and the Royal Society. The operation of all tall tower stations was funded by BEIS through contract GA01103. The ChemSonde work at Cambridge also funded under NERC grant number NERC NE/K005855/1.

#### Appendix A: Tall Tower Site Descriptions

760 Table 1 describes the basic characteristics of each site. The MHD atmospheric research station is situated on the west coast of Ireland. MHD receives well-mixed air masses from prevailing south-westerly winds across the North Atlantic (on average 37% of the time (Grant et al., 2010)), providing a good mid-latitude Northern Hemisphere background signal. The resulting timeseries provides an essential baseline for the combined UK GHG measurement network. The area immediately surrounding MHD is generally wet, boggy with areas of exposed rock and is sparsely populated with  
765 very low associated anthropogenic emissions (Dimmer et al., 2001). The closest city to MHD is Galway, which lies 55 km east of MHD and has a population of 75,000.

RGL is a rural UK site located 30 km from the border of England and Wales. It is 16 km southeast of Hereford (population 55,800), and 30 km southwest of Worcester (population 98,800), in Herefordshire, UK (Office for National Statistics, 2012). The land surrounding the tower is primarily used for arable, livestock and mixed farming purposes (Department of the Environment and Rural Affairs, 2010a). There are 25 wastewater treatment plants within a 40 km radius of the site, the majority of which are in the northeast to southeasterly wind sector (Department of the Environment and Rural Affairs, 2010b). A landfill site lies 30 km to the east of the site.

775 TAC is a rural UK site located near the east coast of England. It is 16 km southwest of Norwich (population 200,000), and 28 km east of Thetford (population 20,000), in Norfolk, UK (Office for National Statistics, 2012). Land surrounding the tower is primarily used for agriculture, which is dominated by arable farming (Department of the Environment and Rural Affairs, 2010a). There are three landfill sites between 30 and 50 km from the site, the closest being 30 km to the east (NCC,  
780 2013). There is also a poultry litter power station in Eye, 20 km south of the site (Energy Power Resources Ltd., 2013).

TTA is a rural UK site located near the east coast of Scotland. It is 10 km north of Dundee (population 148,000 (General Register Office for Scotland, 2013)). Land surrounding the tower is predominantly under agricultural use, primarily livestock farming due to its hilly terrain.

785 HFD is located in rural East Sussex, 20 km from the coast surrounded by woodland, parkland and agricultural green space. The closest large conurbation, Royal Tunbridge Wells (district population



264,000 (Office for National Statistics, 2012)), is located 17km NNE from the tower, while greater London is 40 km NNE.

BSD is a remote moorland plateau site within the North Yorkshire Moors National Park. It is 25km  
790 NNW of Middlesbrough (the closest large urban area, population 139,000 (Office for National Statistics, 2012)) and 30km from the coast.





## References

- Norfolk County Council, Landfill Sites location, <https://goo.gl/8BkGB4>, accessed on 8th August 2013, 2013.
- Alexe, M., Bergamaschi, P., Segers, A., Detmers, R., Butz, A., Hasekamp, O., Guerlet, S., Parker, R., Boesch,  
795 H., Frankenberg, C., Scheepmaker, R. A., Dlugokencky, E., Sweeney, C., Wofsy, S. C., and Kort, E. A.:  
Inverse modelling of CH<sub>4</sub> emissions for 2010–2011 using different satellite retrieval products from  
GOSAT and SCIAMACHY, *Atmospheric Chemistry and Physics*, 15, 113–133, doi:10.5194/acp-15-113-  
2015, <https://www.atmos-chem-phys.net/15/113/2015/>, 2015.
- Allen, G.: Feasibility of aerial measurements of methane emissions from landfills, Tech. Rep. SC130034/R,  
800 Environment Agency, ISBN 978-1-84911-329-8, 2014.
- Allen, G., Coe, H., Clarke, A., Bretherton, C., Wood, R., Abel, S. J., Barrett, P., Brown, P., George, R., Fre-  
itag, S., McNaughton, C., Howell, S., Shank, L., Kapustin, V., Brekhovskikh, V., Kleinman, L., Lee, Y.-N.,  
Springston, S., Toniazzi, T., Krejci, R., Fochesatto, J., Shaw, G., Krecl, P., Brooks, B., McMeeking, G.,  
Bower, K. N., Williams, P. I., Crosier, J., Crawford, I., Connolly, P., Allan, J. D., Covert, D., Bandy, A. R.,  
805 Russell, L. M., Trembath, J., Bart, M., McQuaid, J. B., Wang, J., and Chand, D.: South East Pacific atmo-  
spheric composition and variability sampled along 20°S during VOCALS-REx, *Atmospheric Chemistry and  
Physics*, 11, 5237–5262, doi:10.5194/acp-11-5237-2011, <http://www.atmos-chem-phys.net/11/5237/2011/>,  
2011.
- Allen, G., Illingworth, S. M., O’Shea, S. J., Newman, S., Vance, A., Bauguitte, S. J.-B., Marengo, F., Kent, J.,  
810 Bower, K., Gallagher, M. W., Muller, J., Percival, C. J., Harlow, C., Lee, J., and Taylor, J. P.: Atmospheric  
composition and thermodynamic retrievals from the ARIES airborne TIR-FTS system – Part 2: Validation  
and results from aircraft campaigns, *Atmospheric Measurement Techniques*, 7, 4401–4416, doi:10.5194/amt-  
7-4401-2014, <http://www.atmos-meas-tech.net/7/4401/2014/>, 2014.
- Allen, G., Pitt, J., Hollingsworth, P., Mead, I., Kabbabe, K., Roberts, G., and Percival, C.: Measuring landfill  
815 methane emissions using unmanned aerial systems, Tech. Rep. SC140015/R, Environment Agency, ISBN  
978-1-84911-367-0, 2015.
- Allen, G., P. H., Kabbabe, K., Pitt, J., Mead, M., Illingworth, S., Roberts, G., Bourn, M., Shallcross, D., and  
Percival, C.: The development and trial of an unmanned aerial system for the measurement of methane flux  
from landfill and greenhouse gas emission hotspots, *J. Waste Management*, 2017.
- 820 Berhanu, T. A., Szidat, S., Brunner, D., Satar, E., Schanda, R., Nyfeler, P., Battaglia, M., Steinbacher, M., Ham-  
mer, S., and Leuenberger, M.: Estimation of the fossil fuel component in atmospheric CO<sub>2</sub> based on radio-  
carbon measurements at the Beromünster tall tower, Switzerland, *Atmospheric Chemistry and Physics*, 17,  
10753–10766, doi:10.5194/acp-17-10753-2017, <https://www.atmos-chem-phys.net/17/10753/2017/>, 2017.
- Bloom, A. A., Palmer, P. I., Fraser, A., and Reay, D. S.: Seasonal variability of tropical wetland CH<sub>4</sub> emissions:  
825 the role of the methanogen-available carbon pool, *Biogeosciences*, 9, 2821–2830, doi:10.5194/bg-9-2821-  
2012, <https://www.biogeosciences.net/9/2821/2012/>, 2012.
- Brown, E. N., Friehe, C. A., and Lenschow, D. H.: The Use of Pressure Fluctuations on the Nose of an Aircraft  
for Measuring Air Motion, *Journal of Climate and Applied Meteorology*, 22, 171–180, doi:10.1175/1520-  
0450(1983)022<0171:TUOPFO>2.0.CO;2, 1983.



- 830 Clerbaux, C., Boynard, A., Clarisse, L., George, M., Hadji-Lazaro, J., Herbin, H., Hurtmans, D., Pommier, M., Razavi, A., Turquety, S., et al.: Monitoring of atmospheric composition using the thermal infrared IASI/MetOp sounder, *Atmospheric Chemistry and Physics*, 9, 6041–6054, 2009.
- Deng, F., Jones, D. B. A., Henze, D. K., Bousserrez, N., Bowman, K. W., Fisher, J. B., Nassar, R., O'Dell, C., Wunch, D., Wennberg, P. O., Kort, E. A., Wofsy, S. C., Blumenstock, T., Deutscher, N. M., Griffith, D.
- 835 W. T., Hase, F., Heikkinen, P., Sherlock, V., Strong, K., Sussmann, R., and Warneke, T.: Inferring regional sources and sinks of atmospheric CO<sub>2</sub> from GOSAT XCO<sub>2</sub> data, *Atmospheric Chemistry and Physics*, 14, 3703–3727, doi:10.5194/acp-14-3703-2014, <https://www.atmos-chem-phys.net/14/3703/2014/>, 2014.
- Department for Business Energy and Industrial Strategy: 2015 UK Greenhouse Gas Emissions, Final Figures, Online at [https://www.gov.uk/government/uploads/system/uploads/attachment\\_data/file/604350/2015\\_Final\\_Emissions\\_statistics.pdf](https://www.gov.uk/government/uploads/system/uploads/attachment_data/file/604350/2015_Final_Emissions_statistics.pdf),
- 840 2017.
- Department of the Environment and Rural Affairs: County level crop areas/livestock numbers/labour force: 1905-2010, June survey of Agriculture 2010, Tech. rep., Defra, 2010a.
- Department of the Environment and Rural Affairs: Waste water treatment in the United Kingdom-2012: Implementation of the European Union Urban Waste Water treatment directive 91/271/EEC, PB13811, Tech. rep.,
- 845 Defra, 2010b.
- Di Carlo, P., A. E., Busilacchio, M., Giammaria, F., Dari-Salisburgo, C., Biancofiore, F., Visconti, G., Lee, J., Moller, S., E. Reeves, C., Bauguitte, S., Forster, G., L. Jones, R., and Ouyang, B.: Aircraft based four-channel thermal dissociation laser induced fluorescence instrument for simultaneous measurements of NO<sub>2</sub>, total peroxy nitrate, total alkyl nitrate, and HNO<sub>3</sub>, *Atmospheric Measurement Techniques*, doi:10.5194/amt-6-971-2013, 2013.
- 850 Dimmer, C. H., Simmonds, P. G., Nickless, G., and Bassford, M. R.: Biogenic fluxes of halomethanes from Irish peatland ecosystems, *Atmospheric Environment*, 35, 321 – 330, doi:[http://dx.doi.org/10.1016/S1352-2310\(00\)00151-5](http://dx.doi.org/10.1016/S1352-2310(00)00151-5), <http://www.sciencedirect.com/science/article/pii/S1352231000001515>, 2001.
- Emmons, L. K., Walters, S., Hess, P. G., Lamarque, J.-F., Pfister, G. G., Fillmore, D., Granier, C., Guenther, A.,
- 855 Kinnison, D., Laepple, T., Orlando, J., Tie, X., Tyndall, G., Wiedinmyer, C., Baughcum, S. L., and Kloster, S.: Description and evaluation of the Model for Ozone and Related chemical Tracers, version 4 (MOZART-4), *Geoscientific Model Development*, 3, 43–67, doi:10.5194/gmd-3-43-2010, <https://www.geosci-model-dev.net/3/43/2010/>, 2010.
- Energy Power Resources Ltd.: Location of power generation sites, <http://www.eprl.co.uk/assets/eye/overview.html>, 2013.
- 860 Feng, L., Palmer, P. I., Bösch, H., and Dance, S.: Estimating surface CO<sub>2</sub> fluxes from space-borne CO<sub>2</sub> dry air mole fraction observations using an ensemble Kalman Filter, *Atmospheric Chemistry and Physics*, 9, 2619–2633, doi:10.5194/acp-9-2619-2009, 2009.
- Feng, L., Palmer, P. I., Yang, Y., Yantosca, R. M., Kawa, S. R., Paris, J.-D., Matsueda, H., and Machida, T.:
- 865 Evaluating a 3-D transport model of atmospheric CO<sub>2</sub> using ground-based, aircraft, and space-borne data, *Atmospheric Chemistry and Physics*, 11, 2789–2803, doi:10.5194/acp-11-2789-2011, 2011.
- Feng, L., Palmer, P. I., Bösch, H., Parker, R. J., Webb, A. J., Correia, C. S. C., Deutscher, N. M., Domingues, L. G., Feist, D. G., Gatti, L. V., Gloor, E., Hase, F., Kivi, R., Liu, Y., Miller, J. B., Morino, I., Sussmann, R., Strong, K., Uchino, O., Wang, J., and Zahn, A.: Consistent regional fluxes of CH<sub>4</sub> and CO<sub>2</sub> inferred from



- 870 GOSAT proxy XCH<sub>4</sub>:XCO<sub>2</sub> retrievals, 2010–2014, *Atmospheric Chemistry and Physics*, 17, 4781–4797, doi:10.5194/acp-17-4781-2017, <https://www.atmos-chem-phys.net/17/4781/2017/>, 2017.
- Fraser, A., Palmer, P. I., Feng, L., Boesch, H., Cogan, A., Parker, R., Dlugokencky, E. J., Fraser, P. J., Krummel, P. B., Langenfelds, R. L., O'Doherty, S., Prinn, R. G., Steele, L. P., van der Schoot, M., and Weiss, R. F.: Estimating regional methane surface fluxes: the relative importance of surface and GOSAT mole fraction
- 875 measurements, *Atmospheric Chemistry and Physics*, 13, 5697–5713, doi:10.5194/acp-13-5697-2013, <https://www.atmos-chem-phys.net/13/5697/2013/>, 2013.
- Ganesan, A. L., Rigby, M., Zammit-Mangion, A., Manning, A. J., Prinn, R. G., Fraser, P. J., Harth, C. M., Kim, K.-R., Krummel, P. B., Li, S., Mühle, J., O'Doherty, S. J., Park, S., Salameh, P. K., Steele, L. P., and Weiss, R. F.: Characterization of uncertainties in atmospheric trace gas inversions using hierarchical
- 880 Bayesian methods, *Atmospheric Chemistry and Physics*, 14, 3855–3864, doi:10.5194/acp-14-3855-2014, <https://www.atmos-chem-phys.net/14/3855/2014/>, 2014.
- Ganesan, A. L., Manning, A. J., Grant, A., Young, D., Oram, D. E., Sturges, W. T., Moncrieff, J. B., and O'Doherty, S.: Quantifying methane and nitrous oxide emissions from the UK and Ireland using a national-scale monitoring network, *Atmospheric Chemistry and Physics*, 15, 6393–6406, doi:10.5194/acp-15-6393-2015, <http://www.atmos-chem-phys.net/15/6393/2015/>, 2015.
- 885 General Register Office for Scotland: <http://www.gro-scotland.gov.uk/>, 2013.
- Gerbig, C., Schmitgen, S., Kley, D., Volz-Thomas, A., Dewey, K., and Haaks, D.: An improved fast-response vacuum-UV resonance fluorescence CO instrument, *Journal of Geophysical Research: Atmospheres*, 104, 1699–1704, doi:10.1029/1998JD100031, <http://dx.doi.org/10.1029/1998JD100031>, 1999.
- 890 Gerbig, C., Lin, J. C., Wofsy, S. C., Daube, B. C., Andrews, A. E., Stephens, B. B., Bakwin, P. S., and Grainger, C. A.: Toward constraining regional-scale fluxes of CO<sub>2</sub> with atmospheric observations over a continent: 1. Observed spatial variability from airborne platforms, *Journal of Geophysical Research: Atmospheres*, 108, n/a–n/a, doi:10.1029/2002JD003018, <http://dx.doi.org/10.1029/2002JD003018>, 4756, 2003.
- Gerbig, C., Dolman, A. J., and Heimann, M.: On observational and modelling strategies targeted at regional
- 895 carbon exchange over continents, *Biogeosciences*, 6, 1949–1959, doi:10.5194/bg-6-1949-2009, <http://www.biogeosciences.net/6/1949/2009/>, 2009.
- Grant, A., Witham, C. S., Simmonds, P. G., Manning, A. J., and O'Doherty, S.: A 15 year record of high-frequency, in situ measurements of hydrogen at Mace Head, Ireland, *Atmospheric Chemistry and Physics*, 10, 1203–1214, doi:10.5194/acp-10-1203-2010, <http://www.atmos-chem-phys.net/10/1203/2010/>, 2010.
- 900 Graven, H. D., Stephens, B. B., Guilderson, T. P., Campos, T. L., Schimel, D. S., Campbell, J. E., and Keeling, R. F.: Vertical profiles of biospheric and fossil fuel-derived CO<sub>2</sub> and fossil fuel CO<sub>2</sub>: CO ratios from airborne measurements of  $\Delta^{14}\text{C}$ , CO<sub>2</sub> and CO above Colorado, USA, *Tellus B*, 61, 536–546, doi:10.1111/j.1600-0889.2009.00421.x, <http://dx.doi.org/10.1111/j.1600-0889.2009.00421.x>, 2009.
- IPCC: Climate Change 2013: The Physical Science Basis. Contribution of Working Group I to the Fifth Assessment Report of the Intergovernmental Panel on Climate Change, Cambridge University Press, Cambridge, United Kingdom and New York, NY, USA, doi:10.1017/CBO9781107415324, [www.climatechange2013.org](http://www.climatechange2013.org), 2013.
- 905 Jones, A. R., Thomson, D. J., Hort, M., and Devenish, B.: The U.K. Met Office's next-generation atmospheric dispersion model, NAME III, in: *Air Pollution Modeling and its Application XVII (Proceedings of the 27th*



- 910 NATO/CCMS International Technical Meeting on Air Pollution Modelling and its Application), edited by Borrego, C. and Norman, A.-L., pp. 580–589, Springer, 2007.
- Kuze, A., Suto, H., Nakajima, M., and Hamazaki, T.: Initial Onboard Performance of TANSO-FTS on GOSAT, in: Fourier Transform Spectroscopy, p. FTuC2, Optical Society of America, 2009.
- Law, R. M., Matear, R. J., and Francey, R. J.: Comment on "Saturation of the Southern Ocean CO<sub>2</sub> Sink Due to Recent Climate Change", *Science*, 319, 570–570, doi:10.1126/science.1149077, <http://science.sciencemag.org/content/319/5863/570.1>, 2008.
- Levin, I. and Karstens, U.: Inferring high-resolution fossil fuel CO<sub>2</sub> records at continental sites from combined 14CO<sub>2</sub> and CO observations, *Tellus B*, 59, 245–250, doi:10.1111/j.1600-0889.2006.00244.x, <http://dx.doi.org/10.1111/j.1600-0889.2006.00244.x>, 2007.
- 920 Levin, I., Kromer, B., Schmidt, M., and Sartorius, H.: A novel approach for independent budgeting of fossil fuel CO<sub>2</sub> over Europe by 14CO<sub>2</sub> observations, *Geophysical Research Letters*, 30, n/a–n/a, doi:10.1029/2003GL018477, <http://dx.doi.org/10.1029/2003GL018477>, 2194, 2003.
- Lewis, A. C., Evans, M. J., Hopkins, J. R., Punjabi, S., Read, K. A., Purvis, R. M., Andrews, S. J., Moller, S. J., Carpenter, L. J., Lee, J. D., Rickard, A. R., Palmer, P. I., and Parrington, M.: The influence of biomass burning on the global distribution of selected non-methane organic compounds, *Atmospheric Chemistry and Physics*, 13, 851–867, doi:10.5194/acp-13-851-2013, <https://www.atmos-chem-phys.net/13/851/2013/>, 2013.
- 925 Lunt, M. F., Rigby, M., Ganesan, A. L., and Manning, A. J.: Estimation of trace gas fluxes with objectively determined basis functions using reversible-jump Markov chain Monte Carlo, *Geoscientific Model Development*, 9, 3213–3229, doi:10.5194/gmd-9-3213-2016, <https://www.geosci-model-dev.net/9/3213/2016/>, 2016.
- 930 Manizza, M., Keeling, R. F., and Nevison, C. D.: On the processes controlling the seasonal cycles of the air–sea fluxes of O<sub>2</sub> and N<sub>2</sub>O: A modelling study, *Tellus B: Chemical and Physical Meteorology*, 64, 18 429, doi:10.3402/tellusb.v64i0.18429, 2012.
- Manning, A. J., Ryall, D. B., Derwent, R. G., Simmonds, P. G., and O’Doherty, S.: Estimating European emissions of ozone-depleting and greenhouse gases using observations and a modeling back-attribution technique, *Journal of Geophysical Research: Atmospheres*, 108, n/a–n/a, doi:10.1029/2002JD002312, <http://dx.doi.org/10.1029/2002JD002312>, 4405, 2003.
- 935 Manning, A. J., O’Doherty, S., Jones, A. R., Simmonds, P. G., and Derwent, R. G.: Estimating UK methane and nitrous oxide emissions from 1990 to 2007 using an inversion modeling approach, *Journal of Geophysical Research: Atmospheres*, 116, doi:10.1029/2010JD014763, d02305, 2011.
- 940 McNorton, J., Chipperfield, M. P., Gloor, M., Wilson, C., Feng, W., Hayman, G. D., Rigby, M., Krummel, P. B., O’Doherty, S., Prinn, R. G., Weiss, R. F., Young, D., Dlugokencky, E., and Montzka, S. A.: Role of OH variability in the stalling of the global atmospheric CH<sub>4</sub> growth rate from 1999 to 2006, *Atmospheric Chemistry and Physics*, 16, 7943–7956, doi:10.5194/acp-16-7943-2016, <https://www.atmos-chem-phys.net/16/7943/2016/>, 2016.
- 945 Meijer, H. A. J., Smid, H. M., Perez, E., and Keizer, M. G.: Isotopic characterization of anthropogenic CO<sub>2</sub> emissions using isotopic and radiocarbon analysis, *Phys. Chem. Earth*, 21, 483–487, 1996.
- Monks, S. A., Arnold, S. R., Holloway, M. J., Pope, R. J., Wilson, C., Feng, W., Emmerson, K. M., Kerridge, B. J., Latter, B. L., Miles, G. M., Siddans, R., and Chipperfield, M. P.: The TOMCAT global chemical transport model v1.6: description of chemical mechanism and model evaluation, *Geoscientific Model Develop-*



- 950 ment, 10, 3025–3057, doi:10.5194/gmd-10-3025-2017, <https://www.geosci-model-dev.net/10/3025/2017/>, 2017.
- Nordhaus, W. D.: Economic Growth and Climate: The Carbon Dioxide Problem, *The American Economic Review*, 67, 341–346, 1977.
- Office for National Statistics: 2011 Census of England and Wales, 2012.
- 955 Olivier, J. G., Peters, J. A., and Janssens-Maenhout, G.: Trends in global CO<sub>2</sub> emissions 2012 Report, Tech. Rep. RIVM Report 722201002, PBL Netherlands Environmental Assessment Agency, Hague, Neth, 2012.
- Olsen, S. C. and Randerson, J. T.: Differences between surface and column atmospheric CO<sub>2</sub> and implications for carbon cycle research, *Journal of Geophysical Research: Atmospheres*, 109, n/a–n/a, doi:10.1029/2003JD003968, <http://dx.doi.org/10.1029/2003JD003968>, d02301, 2004.
- 960 O’Shea, S. J., Bauguitte, S. J.-B., Gallagher, M. W., Lowry, D., and Percival, C. J.: Development of a cavity-enhanced absorption spectrometer for airborne measurements of CH<sub>4</sub> and CO<sub>2</sub>, *Atmospheric Measurement Techniques*, 6, 1095–1109, doi:10.5194/amt-6-1095-2013, <http://www.atmos-meas-tech.net/6/1095/2013/>, 2013.
- Parker, R., Boesch, H., Cogan, A., Fraser, A., Feng, L., Palmer, P. I., Messerschmidt, J., Deutscher, N., Griffith, D. W., Notholt, J., et al.: Methane observations from the Greenhouse Gases Observing SATellite: Comparison to ground-based TCCON data and model calculations, *Geophysical Research Letters*, 38, 2011.
- 965 Parker, R. J., Boesch, H., Byckling, K., Webb, A. J., Palmer, P. I., Feng, L., Bergamaschi, P., Chevallier, F., Notholt, J., Deutscher, N., Warneke, T., Hase, F., Sussmann, R., Kawakami, S., Kivi, R., Griffith, D. W. T., and Velasco, V.: Assessing 5 years of GOSAT Proxy XCH<sub>4</sub> data and associated uncertainties, *Atmospheric Measurement Techniques*, 8, 4785–4801, doi:10.5194/amt-8-4785-2015, <https://www.atmos-meas-tech.net/8/4785/2015/>, 2015.
- 970 Patra, P. K., Houweling, S., Krol, M., Bousquet, P., Belikov, D., Bergmann, D., Bian, H., Cameron-Smith, P., Chipperfield, M. P., Corbin, K., Fortems-Cheiney, A., Fraser, A., Gloor, E., Hess, P., Ito, A., Kawa, S. R., Law, R. M., Loh, Z., Maksyutov, S., Meng, L., Palmer, P. I., Prinn, R. G., Rigby, M., Saito, R., and Wilson, C.: TransCom model simulations of CH<sub>4</sub> and related species: linking transport, surface flux and chemical loss with CH<sub>4</sub> variability in the troposphere and lower stratosphere, *Atmospheric Chemistry and Physics*, 11, 12813–12837, doi:10.5194/acp-11-12813-2011, <https://www.atmos-chem-phys.net/11/12813/2011/>, 2011.
- Petersen, G. N. and Renfrew, I. A.: Aircraft-based observations of air–sea fluxes over Denmark Strait and the Irminger Sea during high wind speed conditions, *Quarterly Journal of the Royal Meteorological Society*, 980 135, 2030–2045, doi:10.1002/qj.355, <http://dx.doi.org/10.1002/qj.355>, 2009.
- Pitt, J. R., LeÂ Breton, M., Allen, G., Percival, C. J., Gallagher, M. W., Bauguitte, S. J.-B., O’Shea, S. J., Muller, J. B. A., Zahniser, M. S., Pyle, J., and Palmer, P. I.: The development and evaluation of airborne in situ N<sub>2</sub>O and CH<sub>4</sub> sampling using a quantum cascade laser absorption spectrometer (QCLAS), *Atmospheric Measurement Techniques*, 9, 63–77, doi:10.5194/amt-9-63-2016, 985 <https://www.atmos-meas-tech.net/9/63/2016/>, 2016.
- Polson, D., Fowler, D., Nemitz, E., Skiba, U., McDonald, A., Famulari, D., Marco, C. D., Simmons, I., Weston, K., Purvis, R., Coe, H., Manning, A., Webster, H., Harrison, M., O’Sullivan, D., Reeves, C., and Oram, D.: Estimation of spatial apportionment of greenhouse gas emissions for the UK using boundary layer measurements and inverse modelling technique, *Atmospheric Environment*, 45, 1042 –



- 990 1049, doi:<https://doi.org/10.1016/j.atmosenv.2010.10.011>, <http://www.sciencedirect.com/science/article/pii/S1352231010008733>, 2011.
- Riddick, S., Hancock, B., Robinson, A., Connors, S., Davies, S., Allen, G., Pitt, J., and Harris, N.: Development of a low-maintenance measurement approach to continuously estimate methane emissions: A case study, *Waste Management*, doi:<https://doi.org/10.1016/j.wasman.2016.12.006>, <http://www.sciencedirect.com/science/article/pii/S0956053X16307449>, 2016.
- 995 Riddick, S. N., Connors, S., Robinson, A. D., Manning, A. J., Jones, P. S. D., Lowry, D., Nisbet, E., Skelton, R. L., Allen, G., Pitt, J., and Harris, N. R. P.: Estimating the size of a methane emission point source at different scales: from local to landscape, *Atmospheric Chemistry and Physics*, 17, 7839–7851, doi:10.5194/acp-17-7839-2017, <https://www.atmos-chem-phys.net/17/7839/2017/>, 2017.
- 1000 Roberts, M. L. and Southon, J. R.: A preliminary determination of the absolute  $^{14}\text{C}/^{12}\text{C}$  ratio of OX-1, *Radio-carbon*, 49, 441–445, 2007.
- Saikawa, E., Prinn, R. G., Dlugokencky, E., Ishijima, K., Dutton, G. S., Hall, B. D., Langenfelds, R., Tohjima, Y., Machida, T., Manizza, M., Rigby, M., O'Doherty, S., Patra, P. K., Harth, C. M., Weiss, R. F., Krummel, P. B., van der Schoot, M., Fraser, P. J., Steele, L. P., Aoki, S., Nakazawa, T., and Elkins, J. W.: Global and regional emissions estimates for  $\text{N}_2\text{O}$ , *Atmospheric Chemistry and Physics*, 14, 4617–4641, doi:10.5194/acp-14-4617-2014, <https://www.atmos-chem-phys.net/14/4617/2014/>, 2014.
- 1005 Sander, S. P., Golden, D. M., Kurylo, M. J., Moortgat, G. K., Wine, P. H., Ravishankara, A. R., Kolb, C. E., Molina, M. J., Finlayson-Pitts, B. J., Huie, R. E., and Orkin, V. L.: Chemical kinetics and photochemical data for use in atmospheric studies, Tech. Rep. Evaluation Number 15, JPL Publication06-2, Jet Propul. Lab., Calif. Inst. of Technol., Pasadena, Calif., 2006.
- 1010 Shah, A., Allen, Ricketts, G., H., Williams, P., Kabbabe, K., Hollingsworth, P., Helmore, J., Pitt, J., Bourn, M., Finlayson, A., Robinson, R., Newton, R., Rees-White, T., Beaven, R., and Scheutz, C.: Development of a method for quantifying point-source methane fluxes derived from unmanned aerial vehicle sampling, submitted to *Environmental Science & Technology*, 2017.
- 1015 Siddans, R., Knappett, D., Kerridge, B., Waterfall, A., Hurley, J., Latter, B., Boesch, H., and Parker, R.: Global height-resolved methane retrievals from the Infrared Atmospheric Sounding Interferometer (IASI) on MetOp, *Atmospheric Measurement Techniques*, 10, 4135–4164, doi:10.5194/amt-10-4135-2017, <https://www.atmos-meas-tech.net/10/4135/2017/>, 2017.
- Sonderfeld, H., Bösch, H., Jeanjean, A. P. R., Riddick, S. N., Allen, G., Ars, S., Davies, S., Harris, N., Humpage, N., Leigh, R., and Pitt, J.:  $\text{CH}_4$  emission estimates from an active landfill site inferred from a combined approach of CFD modelling and in situ FTIR measurements, *Atmospheric Measurement Techniques*, 10, 3931–3946, doi:10.5194/amt-10-3931-2017, <https://www.atmos-meas-tech.net/10/3931/2017/>, 2017.
- 1020 Stanley, K. M., Grant, A., O'Doherty, S., Young, D., Manning, A. J., Stavert, A. R., Spain, T. G., Salameh, P. K., Harth, C. M., Simmonds, P. G., Sturges, W. T., Oram, D. E., and Derwent, R. G.: Greenhouse gas measurements from a UK network of tall towers: technical description and first results, *Atmospheric Measurement Techniques Discussions*, 2017, 1–43, doi:10.5194/amt-2017-349, <https://www.atmos-meas-tech-discuss.net/amt-2017-349/>, 2017.
- 1025



- Stein, A. F., Draxler, R. R., Rolph, G. D., Stunder, B. J. B., Cohen, M. D., and Ngan, F.: NOAA's HYSPLIT Atmospheric Transport and Dispersion Modeling System, *Bulletin of the American Meteorological Society*, 1030 96, 2059–2077, doi:10.1175/BAMS-D-14-00110.1, <https://doi.org/10.1175/BAMS-D-14-00110.1>, 2015.
- Ström, J., Busen, R., Quante, M., Guillemet, B., Brown, P. R. A., and Heintzenberg, J.: Pre-EUCREX Intercomparison of Airborne Humidity Measuring Instruments, *Journal of Atmospheric and Oceanic Technology*, 11, 1392–1399, doi:10.1175/1520-0426(1994)011<1392:PEIOAH>2.0.CO;2, 1994.
- Takahashi, T., Sutherland, S. C., Wanninkhof, R., Sweeney, C., Feely, R. A., Chipman, D. W., Hales, B., 1035 Friederich, G., Chavez, F., Sabine, C., Watson, A., Bakker, D. C., Schuster, U., Metzl, N., Yoshikawa-Inoue, H., Ishii, M., Midorikawa, T., Nojiri, Y., Körtzinger, A., Steinhoff, T., Hoppema, M., Olafsson, J., Arnarson, T. S., Tilbrook, B., Johannessen, T., Olsen, A., Bellerby, R., Wong, C., Delille, B., Bates, N., and de Baar, H. J.: Climatological mean and decadal change in surface ocean pCO<sub>2</sub>, and net sea–air CO<sub>2</sub> flux over the global oceans, *Deep Sea Research Part II: Topical Studies in Oceanography*, 56, 1040 554 – 577, doi:<https://doi.org/10.1016/j.dsr2.2008.12.009>, <http://www.sciencedirect.com/science/article/pii/S0967064508004311>, surface Ocean CO<sub>2</sub> Variability and Vulnerabilities, 2009.
- Thompson, R. L., Ishijima, K., Saikawa, E., Corazza, M., Karstens, U., Patra, P. K., Bergamaschi, P., Chevalier, F., Dlugokencky, E., Prinn, R. G., Weiss, R. F., O'Doherty, S., Fraser, P. J., Steele, L. P., Krummel, P. B., Vermeulen, A., Tohjima, Y., Jordan, A., Haszpra, L., Steinbacher, M., Van der Laan, S., Aalto, T., 1045 Meinhardt, F., Popa, M. E., Moncrieff, J., and Bousquet, P.: TransCom N<sub>2</sub>O model inter-comparison Part 2: Atmospheric inversion estimates of N<sub>2</sub>O emissions, *Atmospheric Chemistry and Physics*, 14, 6177–6194, doi:10.5194/acp-14-6177-2014, <https://www.atmos-chem-phys.net/14/6177/2014/>, 2014.
- Thoning, K. W., Tans, P. P., and Komhyr, W. D.: Atmospheric carbon dioxide at Mauna Loa Observatory: 2. Analysis of the NOAA GMCC data, 1974–1985, *Journal of Geophysical Research: Atmospheres*, 94, 8549– 1050 8565, doi:10.1029/JD094iD06p08549, <http://dx.doi.org/10.1029/JD094iD06p08549>, 1989.
- Turnbull, J., Rayner, P., Miller, J., Naegler, T., Ciais, P., and Cozic, A.: On the use of <sup>14</sup>CO<sub>2</sub> as a tracer for fossil fuel CO<sub>2</sub>: Quantifying uncertainties using an atmospheric transport model, *Journal of Geophysical Research: Atmospheres*, 114, n/a–n/a, doi:10.1029/2009JD012308, <http://dx.doi.org/10.1029/2009JD012308>, d22302, 2009.
- 1055 Turnbull, J. C., Miller, J. B., Lehman, S. J., Tans, P. P., Sparks, R. J., and Southon, J.: Comparison of <sup>14</sup>CO<sub>2</sub>, CO, and SF<sub>6</sub> as tracers for recently added fossil fuel CO<sub>2</sub> in the atmosphere and implications for biological CO<sub>2</sub> exchange, *Geophysical Research Letters*, 33, n/a–n/a, doi:10.1029/2005GL024213, <http://dx.doi.org/10.1029/2005GL024213>, 101817, 2006.
- van der Werf, G. R., Randerson, J. T., Giglio, L., Collatz, G. J., Mu, M., Kasibhatla, P. S., Morton, D. C., 1060 DeFries, R. S., Jin, Y., and van Leeuwen, T. T.: Global fire emissions and the contribution of deforestation, savanna, forest, agricultural, and peat fires (1997–2009), *Atmospheric Chemistry and Physics*, 10, 11 707–11 735, doi:10.5194/acp-10-11707-2010, <https://www.atmos-chem-phys.net/10/11707/2010/>, 2010.
- Velders, G.: Description of the RIVM 2-dimensional stratosphere model, Tech. Rep. RIVM Report 722201002, 1995.
- 1065 Villani, M. G., Bergamaschi, P., Krol, M., Meirink, J. F., and Dentener, F.: Inverse modeling of European CH<sub>4</sub> emissions: sensitivity to the observational network, *Atmospheric Chemistry and Physics*, 10, 1249–1267, doi:10.5194/acp-10-1249-2010, <https://www.atmos-chem-phys.net/10/1249/2010/>, 2010.



- Wilson, C., Chipperfield, M. P., Gloor, M., and Chevallier, F.: Development of a variational flux inversion system (INVICAT v1.0) using the TOMCAT chemical transport model, *Geoscientific Model Development*, 7, 2485–2500, doi:10.5194/gmd-7-2485-2014, <https://www.geosci-model-dev.net/7/2485/2014/>, 2014.
- 1070 Wilson, C., Gloor, M., Gatti, L. V., Miller, J. B., Monks, S. A., McNorton, J., Bloom, A. A., Basso, L. S., and Chipperfield, M. P.: Contribution of regional sources to atmospheric methane over the Amazon Basin in 2010 and 2011, *Global Biogeochemical Cycles*, 30, 400–420, doi:10.1002/2015GB005300, <http://dx.doi.org/10.1002/2015GB005300>, 2015GB005300, 2016.



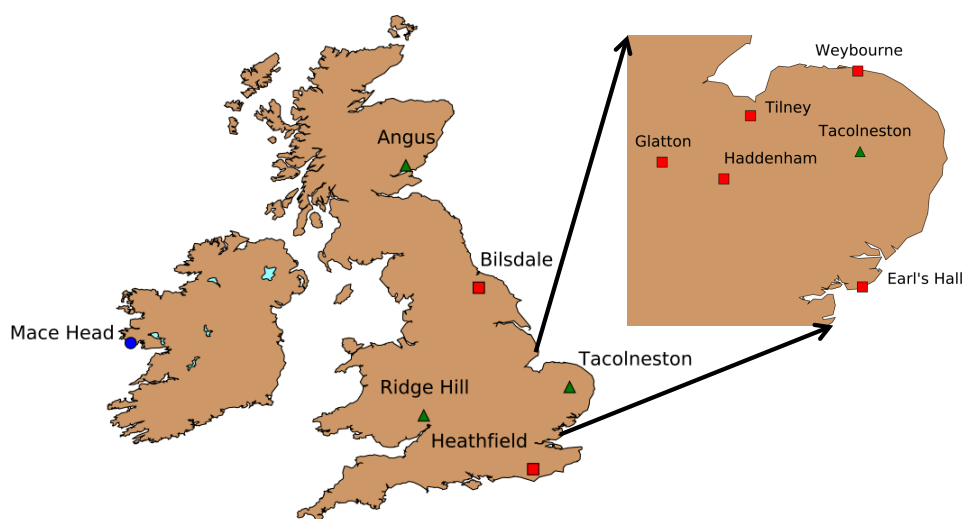


**Figure 1.** The UK DECC network funded by the UK government (sites denoted by green triangles, 2012–), the NERC GAUGE project (denoted by red squares, 2013–2015) and other (blue circle). Sites are described in Table 1 and Appendix A. The enlarged geographical region over East Anglia shows the Church network. These sites are described in Table 4.

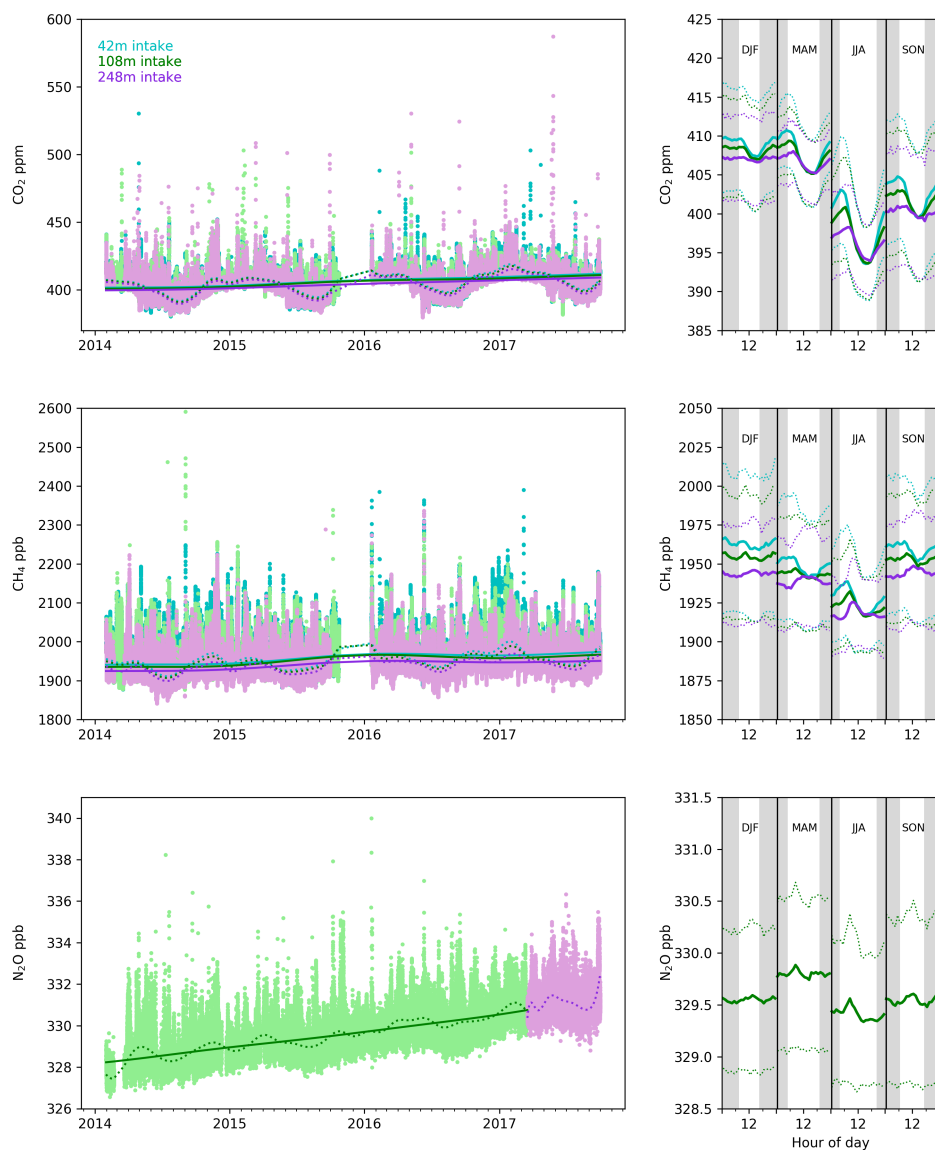


**Figure 2.** Left panels: one-minute mean of CO<sub>2</sub> (ppm), CH<sub>4</sub> (ppb), and N<sub>2</sub>O (ppb) measurements at three inlet heights (42 m, 108 m, and 248 m) at Bilsdale, North Yorkshire from March 2014 to July 2017 (Table 1). The statistical baseline (dashed line) and the long-term trend (solid line) are shown inset for each inlet height. Right panels: mean seasonal diurnal cycle for CO<sub>2</sub>, CH<sub>4</sub>, and CO. The dotted lines denote the ±5th and 95th percentile. Statistical fitting procedures follow Thoning et al. (1989); further details can be found in ARS18a.

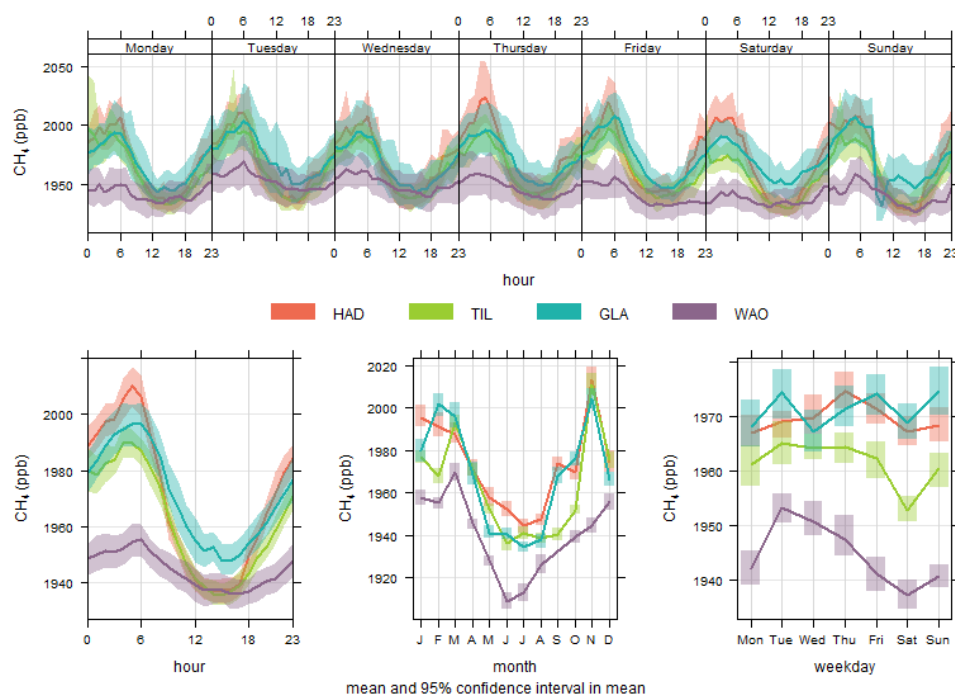


**Figure 3.** Observed variations of  $\text{CH}_4$  mole fraction data collected at one atmospheric observatory (Weyborne, WAO, 13/2/13–6/5/14), and three church steeples at Haddenham (HAD, 3/7/12–23/9/15), Tilney (TIL, 7/6/13–31/8/15), and Glatton (GLA, 22/10/14–5/4/16). The coloured envelope denotes the 95% confidence interval of the hourly, daily, and monthly mean.



**Figure 4.** Photos of the North Sea ferry mobile GHG laboratory on the DFDS Seaways Longstone (now the Finnmerchant). View of the (left) weather station mounted on the top deck and (right) from the air inlet mounted on top of the mobile laboratory located on the weather deck.

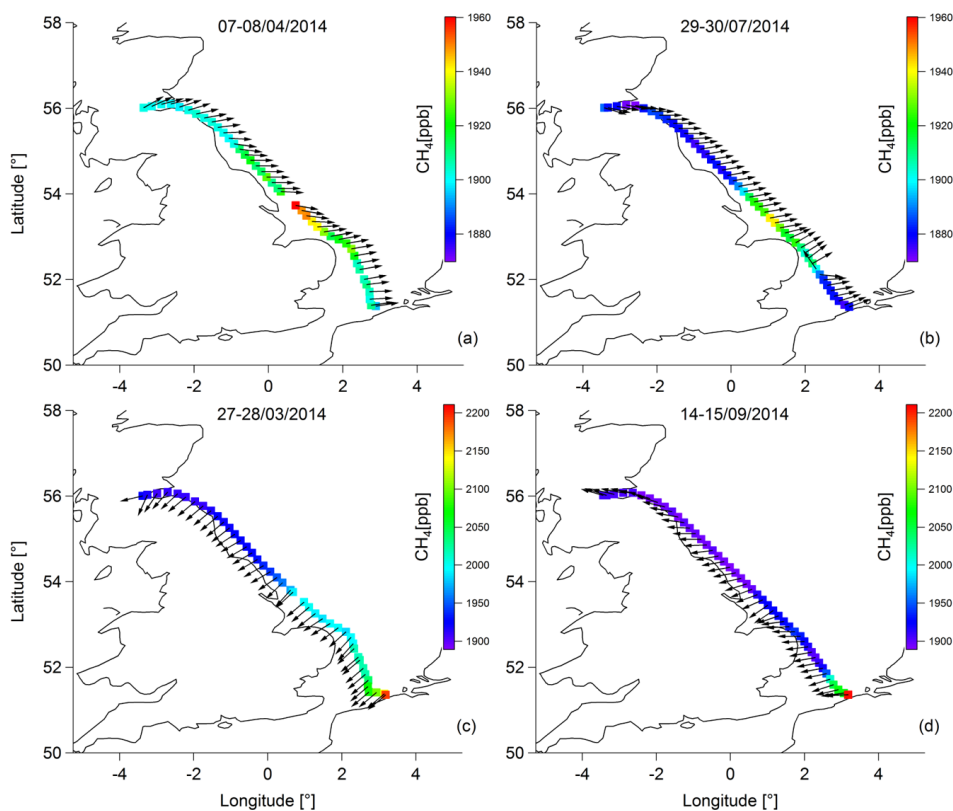


**Figure 5.** Observed temporal and spatial variations in CH<sub>4</sub> mole fractions along the route of the DFDS freight ferry in March, April, July and August 2014. Arrows denote local wind direction.

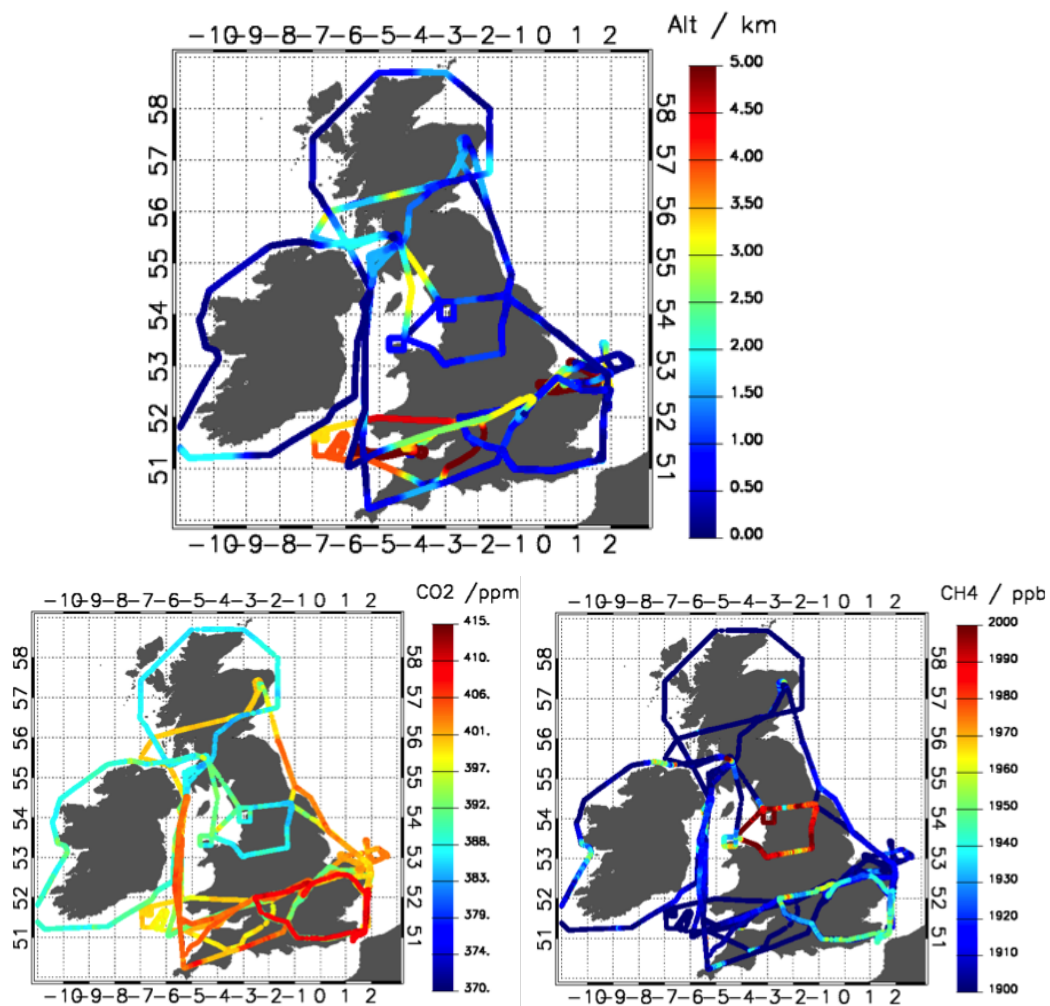


**Figure 6.** Flight tracks for all FAAM flights during GAUGE from 15th May 2014 to 4th April 2016 (Table 6). Colours denote (top) altitude, (bottom left) CO<sub>2</sub> mole fraction, and (bottom right) CH<sub>4</sub> mole fraction. See Table 7 for coincidence comparison between the aircraft and tall tower data.

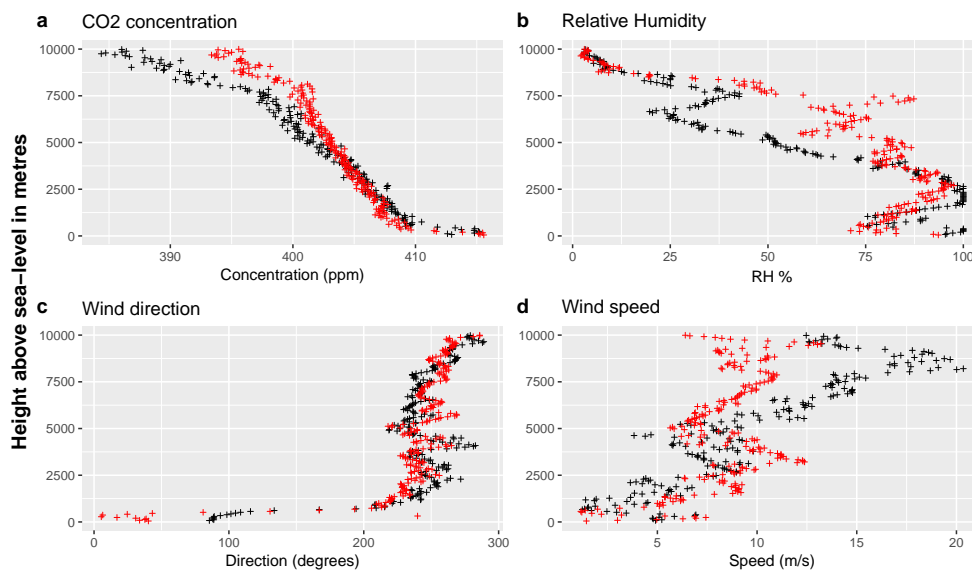


**Figure 7.** Preliminary balloon-borne CO<sub>2</sub> data launched on 14th April, 2016 from Weybourne Atmospheric Observatory UK (Figure 1). Correlative measurements of b) relative humidity, c) windspeed and d) wind direction are also shown. Data are averaged every 10 seconds. Red ticks denote the morning launch and black ticks denote the afternoon launch.

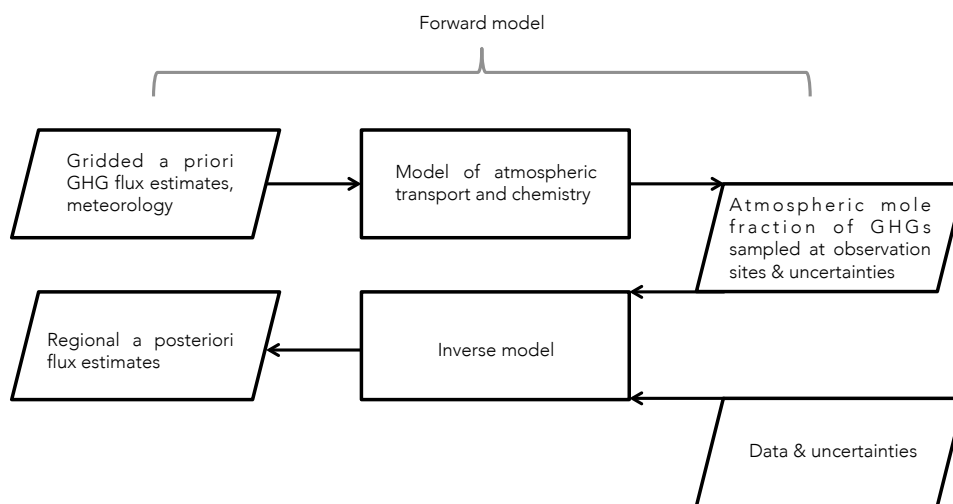


**Figure 8.** Schematic of the generalized GAUGE modelling strategy. The diagram neglects the non-linear inverse modelling approaches.



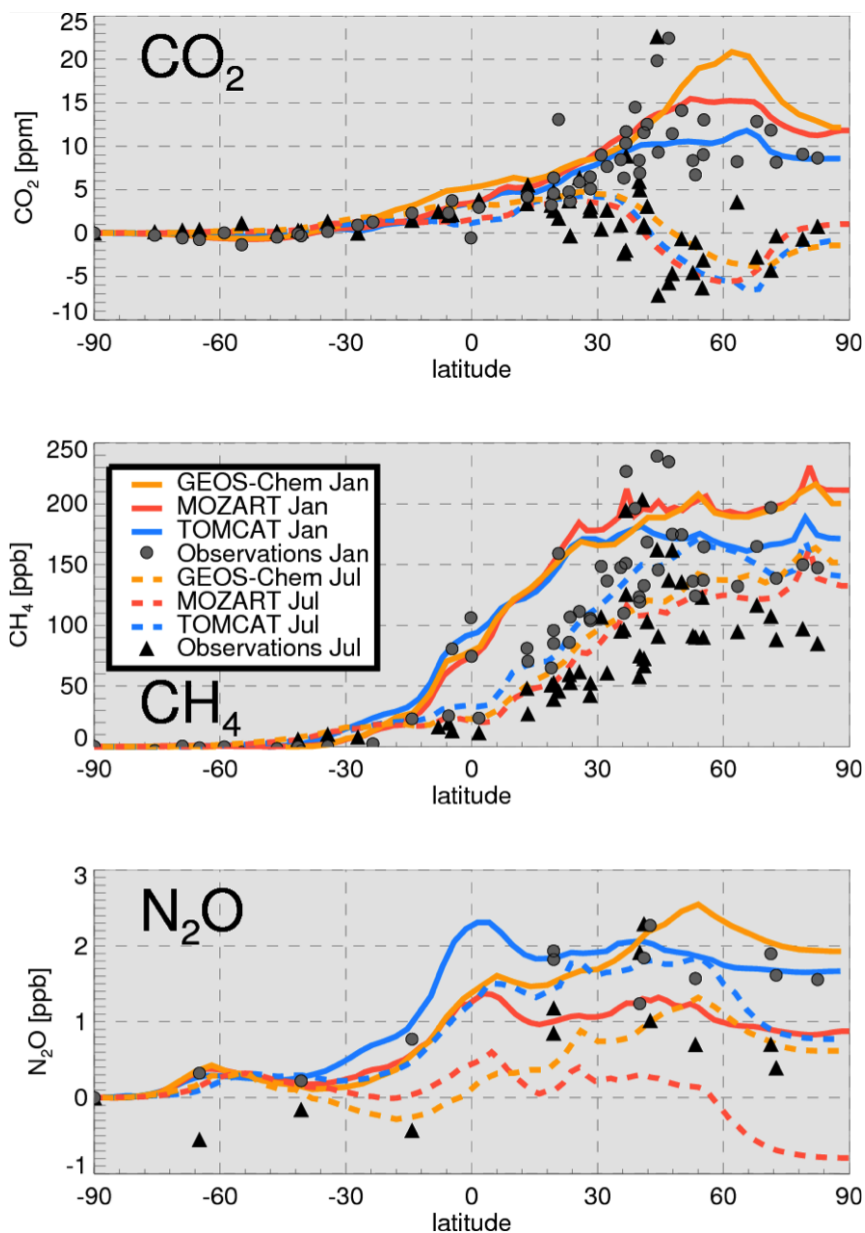


**Figure 9.** Simulated and observed surface zonal mean latitudinal gradient of (a)  $\text{CO}_2$  (ppm); (b)  $\text{CH}_4$  (ppb) and (c)  $\text{N}_2\text{O}$  (ppb) in January (solid lines and circles) and July (dashed lines and triangles), 2011. Observations are made as part of NOAA/ESRL measurement campaign. For each model, its South Pole value is subtracted for all latitudes. Observations are treated similarly.

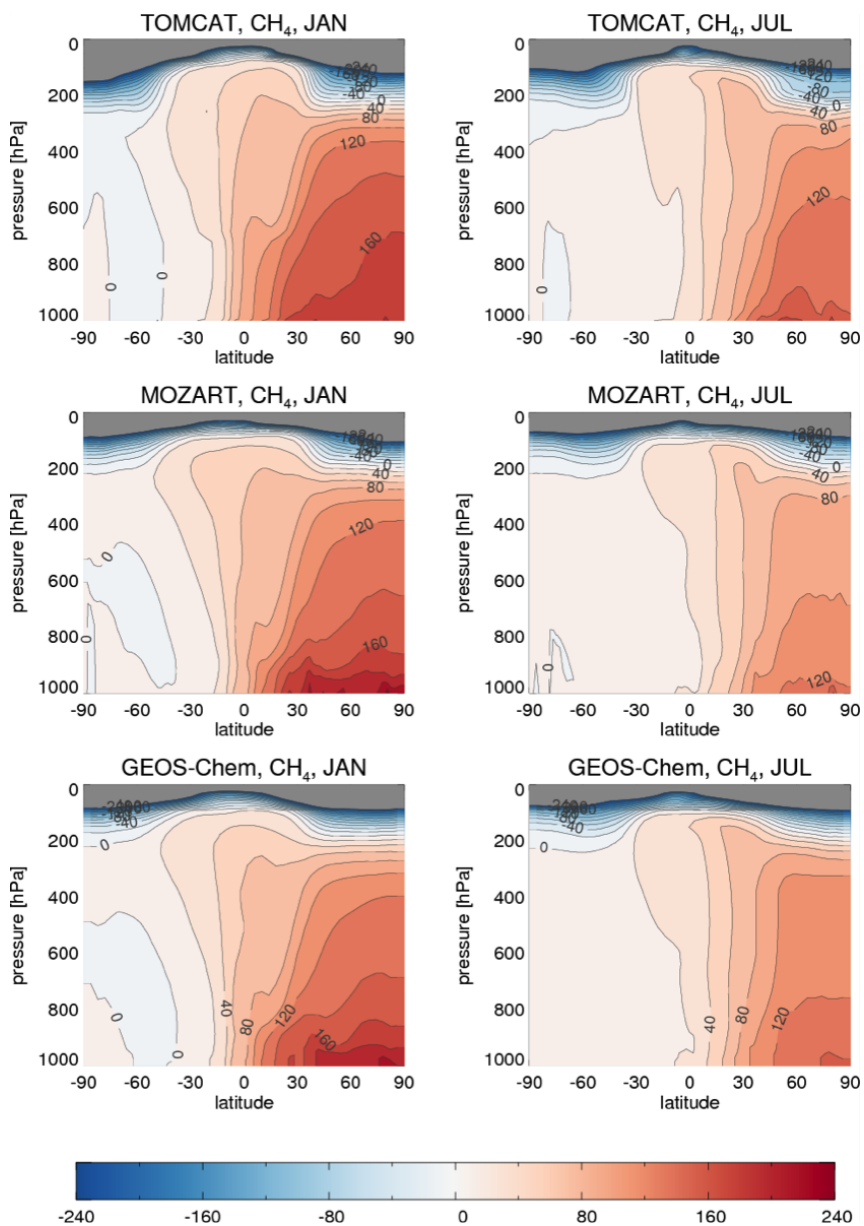


**Figure 10.** Zonal mean distribution of CH<sub>4</sub> (ppb) for January (left column) and July (right column) 2011 in each of the GAUGE CTMs. For each model the concentration of CH<sub>4</sub> at the surface South Pole concentration is subtracted from the global distribution.

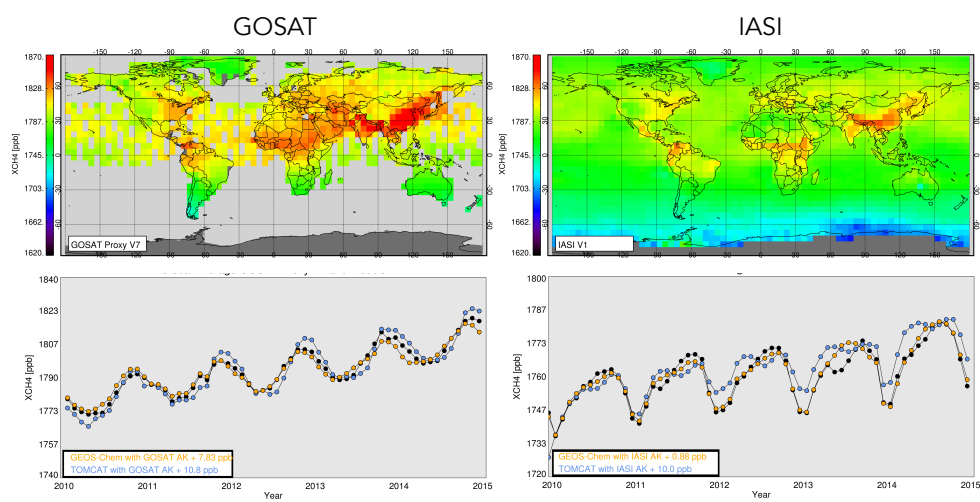


**Figure 11.** Seasonal mean dry air column-averaged mole fractions of  $\text{CH}_4$  ( $\text{XCH}_4$ ) from (top left) GOSAT and (top right) IASI for June–August, 2014, described on a regular  $5^\circ \times 5^\circ$  grid. The bottom rows a global mean time series of  $\text{XCH}_4$  2010–2015. The GEOS-Chem and TOMCAT models have been sampled at the time and location of individual measurements and convolved with scene-dependent averaging kernels prior to calculating the mean value.



**Table 1.** The name, location, and inlet heights of the UK tall tower network. Entries denoted by an asterisk denote an intake used by a GC-MD and, if present at site, by a Medusa GC-MS.

Site Name	Acronym	Location	Start/End Date	Altitude (m.a.s.l.)	Inlet Heights (m.a.g.l.)
Mace Head	MHD	53.327°N 9.904°W	23/01/87–	4	10*
Ridge Hill	RGL	51.998°N 2.540°W	23/02/11–	204	45 & 90*
Tacolneston	TAC	52.518°N 1.139°E	26/07/11–	56	54, 100* & 185
Angus	TTA	56.555°N 2.986°W	13/05/11–29/09/15	400	222
Bilsdale	BSD	54.359°N 1.150°W	30/01/14–	380	42, 108* & 248
Heathfield	HFD	50.977°N 0.231°E	20/11/13–	150	50 & 100*

**Table 2.** Greenhouse gas and ozone depleting substance species and instrumentation at each UK DECC site.

Species	MHD	TAC	RGL	TTA	BIL	HFD
CO <sub>2</sub>	Picarro 2301	Picarro 2301	Picarro 2301	Picarro 2301	Picarro 2401	Picarro 2401
CH <sub>4</sub>	GC-FID	Picarro 2301	Picarro 2301	Picarro 2301	Picarro 2401	Picarro 2401
CO	GC-RGA3	GC-PP1	–	–	Picarro 2401	Picarro 2401
N <sub>2</sub> O	GC-ECD	GC-ECD	GC-ECD	–	GC-ECD	GC-ECD
SF <sub>6</sub>	Medusa GC-MS	GC-ECD	GC-ECD	–	GC-ECD	GC-ECD
		Medusa GC-MS				
H <sub>2</sub>	GC-RGA3	GC-PP1	–	–	–	–
CRDS Nafion drying period	Cryodried, no nafion	Start–19/6/15	Start–6/6/15	11/1/14–End	Start–1/10/15	Start–17/6/15



**Table 3.** Mean seasonal amplitude and mean growth rates of CO<sub>2</sub>, CH<sub>4</sub> and N<sub>2</sub>O at the Bilsdale (BSD), Heathfield (HFD), Ridge Hill (RGL), Tacolneston (TAC), and Angus (TTA) tall tower sites. The mean seasonal amplitude ( $\pm 1$  standard deviation) was calculated from the annual peak-to-peak amplitudes. The mean growth rate is the average of the first derivative of the statistical long-term trend.

	Site	Intake Height (m)	Mean seasonal amplitude (ppm)	Mean growth rate (ppm/yr)
CO <sub>2</sub>	BSD	42	18 $\pm$ 2	3
		108	18 $\pm$ 1	3
		248	18 $\pm$ 1	3
	HFD	50	11 $\pm$ 6	3
		100	13 $\pm$ 5	3
	RGL	45	16 $\pm$ 2	3
		90	17 $\pm$ 2	3
	TAC	54	17 $\pm$ 2	3
		100	18 $\pm$ 2	3
		185	18 $\pm$ 2	2
	TTA	222	16 $\pm$ 1	2
	CH <sub>4</sub>	BSD	42	57 $\pm$ 7
108			56 $\pm$ 2	8
248			41 $\pm$ 4	7
HFD		50	70 $\pm$ 40	6
		100	60 $\pm$ 10	7
RGL		45	70 $\pm$ 20	8
		90	60 $\pm$ 10	8
TAC		54	70 $\pm$ 20	9
		100	70 $\pm$ 20	9
		185	60 $\pm$ 10	8
TTA		222	31 $\pm$ 9	13
N <sub>2</sub> O		BSD	108	0.8 $\pm$ 0.3
	HFD	100	1.0 $\pm$ 0.4	0.9
	RGL	90	1.2 $\pm$ 0.3	0.9
	TAC	100	0.6 $\pm$ 0.3	1.0



**Table 4.** Details of the measurements made in the GAUGE East Anglian network.

Site	Lat [°N], Lon [°E]	Site elevation [m]	Inlet height [m]	Start	End	Measurements	Compounds	Institute lead
Haddenham (HAD)	52.359, 0.148	40	25	07/2012	ongoing	GC-FID	CH <sub>4</sub>	UCAM
Weybourne (WEY)	52.950, 1.122	15	15	02/2013	ongoing	GC-FID	CH <sub>4</sub> , N <sub>2</sub> O	UCAM/UEA
Tilney (TIL)	52.737, 0.321	6	25	06/2013	ongoing	GC-FID	CH <sub>4</sub>	UCAM
Glatton (GLA)	52.461,-0.304	28	20	10/2014	04/2016	<i>in situ</i> FTIR	CH <sub>4</sub> , CO <sub>2</sub> , N <sub>2</sub> O, CO	ULeic
Earls Hall (ELH)	51.813, 1.118	17	50	11/2014	12/2015	CRDS/QCL	CH <sub>4</sub> , CO <sub>2</sub> , N <sub>2</sub> O	UCAM



**Table 5.** Key instrumentation on board the FAAM aircraft for GAUGE-specific flights, including measurement principles and references to instrument characteristics (where available).

Parameter	Technique	Manufacturer/Model	Reference
CO	VUV Fluorescence	Aerolaser, AL5002	Gerbig et al. (1999)
O <sub>3</sub>	UV absorption	Thermo Electron Corporation, 49C	
CH <sub>4</sub> , CO <sub>2</sub>	Off axis-integrated cavity Output spectroscopy	Los Gatos, FGGG 907-0010	O'Shea et al. (2013)
N <sub>2</sub> O, CH <sub>4</sub>	Tunable Infrared Laser	Aerodyne Research, QC-TILDAS-CS	Pitt et al. (2016)
NO <sub>x</sub>	Differential Absorption Spectroscopy		
HFCs, PFCs, SF <sub>6</sub> , C <sub>2</sub> -C <sub>7</sub> VOCs	Chemiluminescence	Air Quality Design	Di Carlo et al. (2013)
Δ <sup>14</sup> CO <sub>2</sub>	Whole air sampling	Thames Restek	Lewis et al. (2013)
δ <sup>13</sup> CH <sub>4</sub>	Glass flask sampling Tedlar bag sampling	NORMAG SKC	
CO <sub>2</sub> , CH <sub>4</sub> , O <sub>3</sub> , H <sub>2</sub> O, CO	FTIR total column remote sensing	UK Met Office, ARIES	Allen et al. (2014)
Humidity	Chilled Mirror	General Eastern, GE 101 IB	Ström et al. (1994)
Temperature	PRT	Rosemount Aerospace, 102 AL	Petersen and Renfrew (2009)
Wind vector	5-hole probe	BAE Systems & UK Met Office	Brown et al. (1983)





**Table 6.** Diary of FAAM survey flights for GAUGE between May 2015 and March 2016, including take-off and landing times; and sampling locations and brief description of mission profiles.

Flight No.	Date	Take-off (UTC)	Landing (UTC)	Description
B848	15/05/14	12:07:07	16:46:25	North Sea Gas Rigs (+instrument test flight)
B849	16/05/14	09:33:16	12:45:28	Bristol Channel (+instrument test flight)
B850	21/05/14	07:59:54	15:22:59	Around Britain – UK outflow
B851	17/06/14	09:56:43	14:43:25	Southwest Approaches – UK inflow
B852	18/06/14	08:25:01	16:29:35	Around Britain – DECC Tower survey
B861	09/07/14	08:55:32	13:20:52	Around London – mass balancing
B862	15/07/14	10:59:32	15:17:35	Around London – mass balancing
B864	01/09/14	08:09:57	10:49:27	Irish Sea – transit to Prestwick
B865	01/09/14	13:03:45	15:51:41	Around Scotland – mass balancing
B866	02/09/14	08:08:16	12:01:38	Around Ireland – mass balancing
B867	02/09/14	13:24:29	17:11:09	Around Ireland – area survey
B868	04/09/14	11:57:58	16:40:22	Northwest England – sources of 14C
B905	12/05/15	07:59:00	11:34:02	Irish Sea SW Approaches – upwind of UK
B906	12/05/15	13:09:14	17:03:19	North Sea – UK outflow
B911	28/05/15	07:55:04	10:19:26	Around Britain – aborted (instrument fault)
B948	04/03/16	08:55:20	14:10:19	Around London – mass balancing



**Table 7.** Comparison between aircraft and ground-based one-minute mean measurements for CO<sub>2</sub> and CH<sub>4</sub> during tall tower fly pasts.

Flight	Station	Inlet altitude (m a.s.l.)	Aircraft Altitude (m a.s.l.)	Tall tower data		Aircraft minus tall tower data	
				CO <sub>2</sub> (ppm)	CH <sub>4</sub> (ppb)	CO <sub>2</sub> (ppm)	CH <sub>4</sub> (ppb)
B850	TTA	522	1022	399.38	1913.99	1.39	5.50
B852	TTA	522	1039	397.37	1908.83	2.26	-58.32
	BSD	488	738	398.05	1878.45	0.11	-1.10
B861	RGL	290	576	390.22	1912.52	2.50	-1.48
	HFD	250	687	402.17	1945.77	-0.23	-9.49
	TAC	104	683	388.57	1876.77	5.86	12.28
	RGL	290	488	390.88	1901.85	-0.15	1.34
	HFD	250	465	395.18	1920.95	1.07	-1.38
B862	TAC	104	675	390.66	1876.53	4.53	13.71
	RGL	290	440	388.84	1891.37	1.00	-4.30
	HFD	200	425	392.88	1869.02	-0.14	1.22
	RGL	290	482	389.31	1886.66	-0.25	1.71
	HFD	200	690	392.93	1874.60	0.77	0.70
B865	TAC	235	373	393.56	1900.04	-3.32	-6.64
	TTA	522	687	384.72	1891.21	0.09	1.37
B866	MHD	29	119	387.63	1891.53	0.34	3.54
B867	MHD	29	105	389.34	1913.09	1.48	11.91
B868	BSD	628	708	386.32	1987.75	0.13	-0.51
	BSD	628	569	384.82	1980.36	0.25	-0.81
B905	RGL	290	431	404.32	1911.47	-0.40	3.48
	RGL	245	457	401.83	1909.53	1.48	-1.06
B906	TAC	104	275	401.13	1912.96	0.13	-2.36
	TAC	150	296	399.85	1913.34	0.09	1.04
B911	RGL	290	713	403.49	1914.23	0.62	1.62
B948	RGL	245	405	409.10	1946.96	0.61	-2.00
	HFD	250	346	411.39	1951.87	-0.86	-2.84
	TAC	104	406	408.86	1942.21	0.07	-0.04
<b>Average</b>						<b>0.72</b>	<b>-1.22</b>
<b>Standard Deviation</b>						<b>1.69</b>	<b>12.54</b>



**Table 8.** Summary of successful ChemSonde launches from Weybourne Atmospheric Observatory.

Instrument #	Launch date/time (UTC)	Altitude/Distance	Comments
709D	14th April, 10:39	33.5/40.2 km	Successful launch: CO <sub>2</sub> and meteorology data.
7097	14th April, 14:30	34.2/43.3 km	Successful launch: CO <sub>2</sub> and meteorological data.



**Table 9.** Model descriptions used in the GAUGE inter-comparison.

Model	Institute	Forward Model Type	Horizontal (Nested) Resolution	Vertical Resolution	Meteorology	Inverse Method	Key References
GEOS-Chem	U. Edinburgh	E	$2^\circ \times 2.5^\circ$ ( $0.25^\circ \times 0.3125^\circ$ )	47 levels (surface to 0.01 hPa)	NASA GEOS-5	EnKF	Feng et al. (2009, 2011, 2017)
MOZART	U. Bristol	E	$2.5^\circ \times 1.9^\circ$	56 levels (surface to 1.65 hPa)	NASA GEOS-5	4D-Var	Emmons et al. (2010)
TOMCAT	U. Leeds	E	$1.125^\circ \times 1.125^\circ$	60 levels (surface to 0.1 hPa)	ECMWF ERA Interim	4D-Var	Wilson et al. (2014); McNorton et al. (2016); Monks et al.
NAME	Met Office/ U. Bristol	L	1.5 km over UK domain	60 levels (surface to 29 km)	Met. Office	Bayesian inference	Manning et al. (2011); Ganesan et al. (2015)